CHALMERS
UNIVERSITY OF TECHNOLOGY

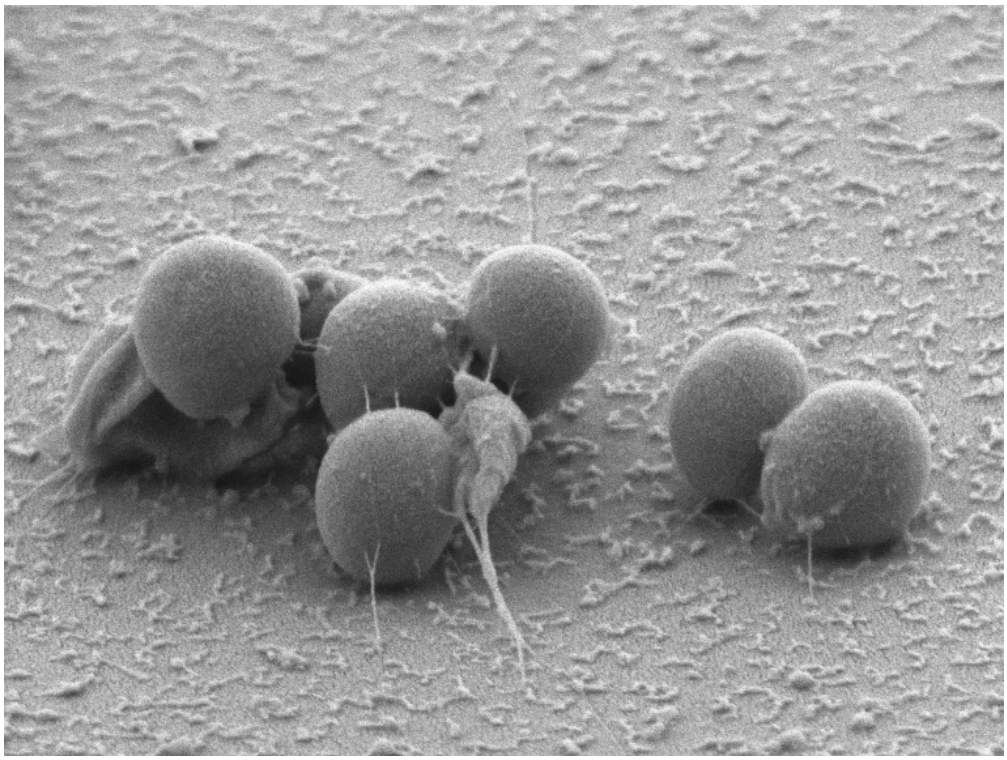

# Combining Photothermal Gold Nanorods and Antibiotics for Treatment of Implant-Associated Infections

## Evaluating if a synergistic effect can be achieved between photothermal gold nanorods and antibiotics

Master's thesis in Materials Chemistry

Ellen Iwarsson

**Department of Chemistry and Chemical Engineering**
CHALMERS UNIVERSITY OF TECHNOLOGY
Gothenburg, Sweden 2023
www.chalmers.se

Master's thesis 2023

# Combining Photothermal Gold Nanorods and Antibiotics for Treatment of Implant-Associated Infections

Evaluating if a synergistic effect can be achieved between photothermal gold nanorods and antibiotics

Ellen Iwarsson


CHALMERS
UNIVERSITY OF TECHNOLOGY

Department of Chemistry and Chemical Engineering
*Division of Applied Chemistry*
M. A. Research Group
Chalmers University of Technology
Gothenburg, Sweden 2023

Combining Photothermal Gold Nanorods and Antibiotics for Treatment of Implant-Associated Infections
Evaluating if a synergistic effect can be achieved between photothermal gold nanorods and antibiotics
ELLEN IWARSSON



Supervisor: Maja Uusitalo, Department of Chemistry and Chemical Engineering
Examiner: Martin Andersson, Department of Chemistry and Chemical Engineering

Master's Thesis 2023
Department of Chemistry and Chemical Engineering
Division of Applied Chemistry
M. A. Research Group
Chalmers University of Technology
SE-412 96 Gothenburg
Telephone +46 31 772 1000

Cover: SEM micrograph visualising a gold nanorod-functionalised glass surface with cultivated *Staphylococcus Aureus* with magnification 40 000x.

Typeset in LaTeX
Printed by Chalmers Reproservice
Gothenburg, Sweden 2023

Combining Photothermal Gold Nanorods and Antibiotics for Treatment of Implant-Associated Infections
Evaluating if a synergistic effect can be achieved between photothermal gold nanorods and antibiotics
ELLEN IWARSSON
Department of Chemistry and Chemical Engineering
Chalmers University of Technology

# Abstract

Implant-associated infections commonly require repeated treatment and high dosages of antibiotics. Being able to effectively treat implant-associated infections is therefore critical for the future of medical implants as well as being able to decrease the usage of antibiotics. This thesis therefore considers a possible alternative to decrease the usage of antibiotics and to more effectively treat implant-associated infections by combining photothermal gold nanorods and antibiotics to achieve a synergistic effect. A procedure has been developed to enable evaluation of the antimicrobial activity and synergistic effect of the combination of photothermal gold nanorods and antibiotics by *In-Vitro* studies. Before performing the *In-Vitro* studies were gold nanorods synthesised with dimensions enabling emission of photothermal heat when exposed to near-infrared (NIR) light, heat which can be used for photothermal elimination of bacteria. The gold nanorods were thereafter immobilised on glass substrates by electrostatic interaction, mimicking a gold nanorod-functionalised implant surface.

The gold nanorod-functionalised substrates were thereafter implemented in the *In-Vitro* studies to evaluate the antimicrobial activity of the gold nanorods exposed to NIR-light. An antimicrobial effect could be achieved when the substrates were exposed to NIR-light covered with a thin liquid film meanwhile no antimicrobial effect could be achieved when the substrates were exposed to NIR-light while immersed in liquid. The antimicrobial activity of vancomycin was also evaluated by minimum inhibitory concentration (MIC) determinations where the MIC for planktonic bacteria and bacteria cultivated on gold nanorod-functionalised substrates were determined. The antimicrobial effect was thereafter evaluated for the combination of gold nanorods exposed to NIR-light and vancomycin. No synergistic effect could be achieved for the parameters considered. No antimicrobial activity nor synergistic effect could therefore be achieved when the gold nanorod-functionalised substrates were irradiated immersed in liquid, with or without antibiotics. The results implicate that more studies are required and that the interaction between the gold nanorods and the bacteria needs to be studied in more detail.

Keywords: Implant-associated infections, synergistic treatment, antibiotics, gold nanorods, gold nanorod-functionalised substrates, photothermal elimination, antimicrobial resistance

# Acknowledgements

Initially I would like to give a special thank you to my examiner Martin Andersson for givning me the opportunity to perform this master thesis and for putting a lot of effort and interest in my project. I would also like to show all my gratitude to my supervisor Maja Uusitalo for her exceptional mentoring, all ideas and hours spent on my project. I would like to show my thankfulness to Mats Hulander and Annija Stepulane who has answered my question about everything from nanoparticles to microbiology. Thanks as well to the whole M. A Research Group for giving me the opportunity of being a part of your wonderful team. At last I want to thank all my family and friends for their support.

Ellen Iwarsson, Gothenburg, May 2023

# Contents

# List of Figures

# List of Tables

# 1
# Introduction

Implant-associated infections is an advancing problem for modern healthcare since the infections often require repeated treatment and high dosages of antibiotics [1]. Although the infections are treated, the outcome is often that the implant requires replacement, with the new implant having a higher risk of re-infection [2]. Being able to effectively treat infections related to medical implants is therefore critical for their future use. Effective treatment of implant-associated infections is also very critical because of increasing concerns of the antimicrobial resistance [1]. New treatment methods are therefore essential to replace or complement the conventional antibiotic treatment of implant-associated infections.

Implant-associated infections originate from bacterial adhesion on the implant surface [2]. The bacterial growth thereafter increase on the implant surface, creating microcolonies. The microcolonies thereafter grow into macrocolonies which has the ability to produce a polymer matrix consisting of polysaccharides and proteins, to mention a few, which encapsulates the cultivated bacteria. The construct of bacteria enclosed in a biopolymer matrix is referred to as a biofilm. The biofilm is more resilient and decrease the ability of drug penetration which can result in a resilience up to a 1000 times higher towards antibiotics compared to planktonic bacteria [1].

Earlier research has proved that synergy can be achieved between antibiotics and heat to more effectively eradicate bacteria [3–6]. One possible alternative to decrease the use of antibiotics is therefore the combination of antibiotics and gold nanorods, which can photothermally eliminate and/or weaken bacteria cultivated on the implant surface [1]. Because of the nanorods' unique properties can incident light interact with the delocalised valence electrons on the nanorods' surfaces, allowing the rods to emit energy in the form of local heat [7]. If the nanords are immobilised on the surface of a medical implant the heat emission generated from the gold nanorods has the potential to photothermally eliminate and/or weaken bacteria cultivated on the implant surface [1]. Expectantly improving the treatment of implant-associated infections by synergy between the photothermal heat from the gold nanorods and the antibiotics.

Depending on the geometry of the gold nanoparticles they absorb varying wavelengths of light [7]. Gold nanorods have a geometry which enables them to absorb light in the near-infrared (NIR) region, 800-2500 nm [7, 8], which incorporates large parts of the so-called biological-window [9]. The biological-window concerns the wavelengths that have the ability to penetrate water, which imply penetration of hu-

man tissue. Accordingly, the nanorods have the ability of being photothermally activated even though located inside the body since they resonate with light penetrating body tissue [1]. Gold nanorods exposed to NIR-light is therefore a promising alternative in combination with antibiotics to more effectively treat implant-associated infections and decrease the usage of antibiotics.

## 1.1 Aim of the Project

The projects aim is to develop a methodology which enables evaluation of the antimicrobial activity of the combination of gold nanorods exposed to NIR-light and antibiotics as well as being able to decide if a synergistic effect is achieved. The aim therefore also includes the development of strategies which enable the evaluation of the antimicrobial activity of the photothermal gold nanorods exposed to NIR-light and the antibiotics separately. The objectives are thus to synthesise gold nanorods by wet chemistry, with absorption in the biological-window, and thereafter immobilise them on glass substrates with electrostatic surface assembly. The objectives also include evaluation of the antimicrobial activity of gold nanorods exposed to NIR-light and the antibiotics separately as well as their combination, which are to be determined by *In-Vitro* studies.

## 1.2 Limitations

This thesis only include one synthesis procedure to produce gold nanorods, called a seed-mediated synthesis where cetyltrimethylammonium bromide (CTAB) act as capping agent. The synthesised gold nanorods are then going to be surface assembled on glass, for research purposes since UV-Vis-NIR sprectroscopy and microscopy can be performed on transparent substrates. One kind of antibiotic will be implemented during the project named vancomycin which is a valid candidate because of its clinical relevancy and extended use in earlier research. For this project will only *In-Vitro* studies be performed, *In-Vivo* studies will not be executed. For the *In-Vitro* studies the strain *Staphylococcus aureus (S.aureus) CCUG 10778* is going to be utilised because *S. aureus* commonly cause implant-associated infections. Only one laser at 808 nm will be utilised for the *In-Vitro* studies and no other irradiation wavelengths will be considered. For this study are the parameters surface coverage of gold nanorods and the geometry of the gold nanorods going to be constant in theory, to ease interpretation of the results.

# 2
# Theory

## 2.1 Implant-Associated Infections

Implant-associated infections constitute of a category of infections, caused by bacteria, with characteristics depending on site and implant type [2]. Implant-associated infections are generally problematic to treat and often result in the need for replacement of the biomedical device [1]. Implant-associated infections originate from bacterial adhesion on the implant surface, which is prone to adhesion due to its biocompatability [2]. Due to further bacterial growth are microcolonies assembled upon the implant surface and the adhered bacteria initiate the production of a biopolymer matrix consisting of polysaccharides and proteins, among other substances. Ultimately are macrocolonies created in combination with production of the biopolymer matrix, which act as a resilient layer encapsulating the bacteria cultivated upon the biomedical implant. This construct of bacteria enclosed in a biopolymer matrix is referred to as a biofilm. The biofilm's capacity of shielding the bacteria can lead up to 1000 times higher resilience towards antibiotics than planktonic bacteria. Which makes the implant-associated infections challenging to treat [1].

The bacteria most prone to cause implant-associated infections are *S. aureus* and *Staphylococcus epidermidis* (*S. epidermidis*) [10]. Both bacteria colonise human skin where *S. Epidermidis* pathogen which often cause less severe infections compared to *S. aureus* [10, 11]. *S. aureus* and *S. epidermidis* have a tendency of biofilm formation which complicates therapeutic treatment [11]. The bacterial species have a spherical from and assemble in grape-like clusters [10]. *Staphylococci* have a diameter that is around 1 $\mu$m and have a contact area around 0.015 $\mu m^2$ [12, 13].

## 2.2 Antibiotics and Antimicrobial Resistance

Antibiotics are different kinds of substances that are implemented to treat some kinds of bacterial infections, for instance implant-associated infections [1, 14]. There are many different kinds of antibiotics and they have varying usage since not all bacteria are susceptible to one antimicrobial substance only [14]. The different antibiotics have diverse mechanisms to target bacteria. One mechanism that is utilised by many antibiotics is the inhibition of the bacterial cell wall synthesis, which result in an alternation in the cell wall and geometry of the target bacteria, that eventually cause cell lysis.

The emerging problem with antimicrobial resistance is a growing concern for the medical field and today's society [1]. Antimicrobial resistance means that the target bacteria for certain antimicrobial agents develop a resistance against the agent, rendering it ineffective in eradicating or inhibiting the growth of the bacteria [15]. One possible outcome is that the bacterial infection then becomes untreatable since the antibiotics no longer can be utilised as treatment. There are many mechanisms that can cause the bacteria to develop antimicrobial resistance, the two most important are mutation and acquisition of new genetic material. Where the major driving force behind the development of antimicrobial resistance is the overuse of antibiotics. It is therefore of great importance to use antibiotics in a rightful way as well as decreasing the utilisation of these pharmaceuticals. One way of decreasing the usage of antibiotics is to find new approaches for treating bacterial infections, which is a pressing and challenging matter in the field of research [1].

## 2.3 Gold Nanorods

One possible complement when treating implant-associated infections is the usage of gold nanorods attached upon implant surfaces and subsequently irradiated to generate heat in order to achieve an antimicrobial effect [1]. The antimicrobial effect is achieved because the released heat from the nanorods eradicate and/or harm bacteria cultivated on the implant surface. The heat emitted can only be performed by noble metal nanoparticles as they have unique properties not present in their bulk counterparts [16].

### 2.3.1 Localised Surface Plasmon Resonance

Gold nanorods possess photothermal properties because of a phenomenon called localised surface plasmon resonance (LSPR) [16]. The mechanism is only possible for noble metal nanoparticles, for instance gold nanoparticles. The particles need to be metallic since only metals can be described with the free-electron theory [17]. The theory explains the delocalisation of valence electrons for solid metals. The valence electrons act as a gas and move unconstrained towards each other over the metal lattice which for instance provide the material with high thermal and electrical conductivity.

When the nobel metal nanoparticles have dimensions smaller than the mean-free path of the conduction band electrons, the incident light can affect the delocalised electrons to oscillate coherently, which is called a surface plasmon [7, 18]. The oscillations create a charge separation between the conduction band electrons and the core of the nanoparticles meanwhile the repulsion between the electrons forces movement in the opposite direction which contribute to the mutual oscillations [7]. The oscillations have a resonance frequency at a certain wavelength which is referred to as the localised surface plasmon resonance (LSPR). When the incoming electromagnetic wave has equal frequency as the resonance frequency the nanoparticles begin to absorb energy more readily compared to other wavelengths [19]. The absorption of light occurs because of the excitation of the localised surface plasmon at the res-

onance frequency.

The geometry of the nanoparticles is not only responsible for the location of the LSPR but also the amount of plasmon bands in a localised surface plasmon resonance spectrum [16]. For a spherical nanoparticle one band is visible in the spectrum, normally around 500-600 nm [7]. For nanorods, the spectrum has two bands because the electrons can either oscillate in the transverse or the longitudinal direction. The transverse oscillation often equals the spherical absorption around 500-600 nm meanwhile the longitudinal absorption often emerge in the NIR region, which is 800-2500 nm [7, 8]. Figure 2.1 shows a general absorption spectrum for dispersed gold nanorods.

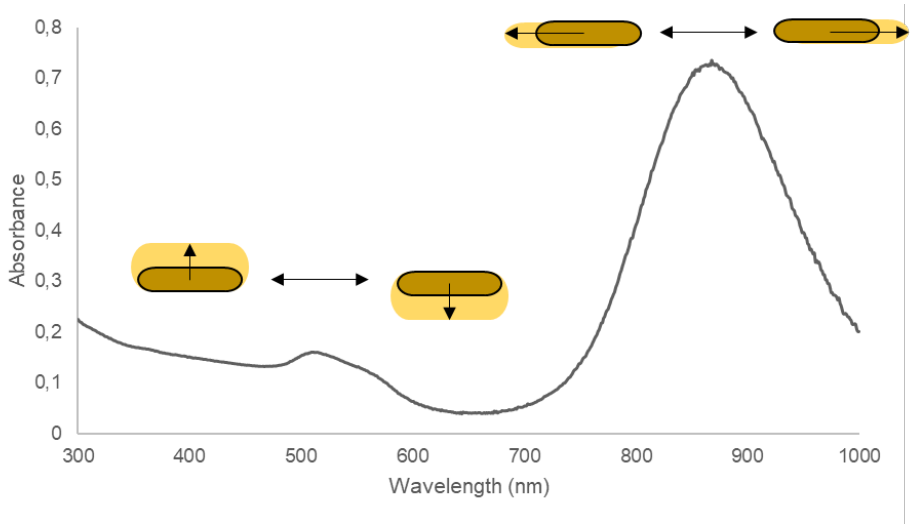


**Figure 2.1:** Localised surface plasmon resonance spectrum which visualises how the absorption of electromagnetic radiation relates to the transverse and longitudinal oscillations of the delocalised valence electrons in a nanorod. The elliptic shapes represent a gold nanorod meanwhile the lighter yellow shapes represent how the valence electrons oscillate.

The transverse oscillations are quite insensitive to shape variation of the nanorods meanwhile the oscillations in the longitudinal direction are shape dependent. The aspect ratio (length/width) decide the exact location of the longitudinal LSPR band [16]. The geometry of the nanorods is therefore utilised to tune the location of the longitudinal absorption band [9]. For biomedical applications is the desired location for the longitudinal absorption band often in the NIR-region. Since wavelengths 700-1200 nm have the ability to penetrate water and therefore also human body tissue, referred to as the "biological window". Radiation can therefore photothermally activate gold nanorods immobilised on implant surfaces inserted into patients' bodies [1].

The localised surface plasmons decay through different processes [20]. One occurs because a part of the absorbed energy is released by electron-phonon collisions providing heat to the nanorod lattice resulting in release of thermal energy to the

surroundings. The heating of the nanorods enables them to be implemented in therapeutic applications since the local heating can weaken and/or eradicate bacteria cultivated on the nanorods [1].

### 2.3.2 Plasmon coupling

Plasmon coupling occurs when gold nanoparticles exists in near vicinity of each other [21]. The plasmons in neighbouring particles then influence one another which change their plasmonic properties. The change in plasmonic properties occur because the particles' electrons start to oscillate not solely over their own lattice structure but also over other praticles lattice structures, creating a shift in the resonance frequency. This phenomena can be both desired and undesired. Plasmon coupling can be utilised in for instance sensor applications but it is of importance to keep in mind that the plasmonic properties of the particles change when they come in close vicinity of one another.

### 2.3.3 Seed-Mediated Synthesis

The synthesis approach utilised to produce the gold nanorods is referred to as a seed-mediated synthesis, since a seed solution and a growth solution is prepared separately [22]. Primarily, nucleation occurs in the seed solution before the seeds are added into the growth solution. The outcome is more homogeneously synthesised nanorods compared to nucleation and growth occurring simultaneously.

Creation of nuclei in the seed solution is accomplished by adding a strongly reducing agent to the gold-precursor ($HAuCl_4$) which induce the nucleation, the reducing agent in this case is $NaBH_4$ [22]. The reducing agent is added in excess during vigorous stirring to achieve uniform nucleation. Cetyltrimethylammonium bromide (CTAB) is present to stabilise the seeds.

The surfactant CTAB is utilised because of its ability to encapsulate both the gold nanorods and the seeds [22], the strucure of CTAB is visualised in figure 2.2. The CTAB capping of the gold nanoparticles during growth favour the formation of rods. On later days conclusions have been drawn that the counterion of bromine plays a key role in the formation of nanorods, since surfactants lacking the bromine counterion make the synthesis unsuccessful. The bromine counterion in CTAB will exchange the $Cl^-$ ions in the gold precursor ($HAuCl_4$) and form complexes with the ammonium surfactant monomers. The ligand exchange and the complex formation affect the growth kinetics and are therefore also thought to be responsible for the production of the nanorods.

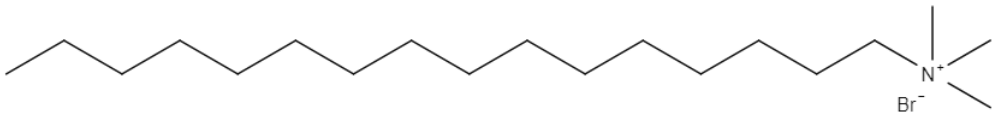


**Figure 2.2:** The molecular structure of CTAB.

Ascorbic acid is added into the growth solution to enable reduction of the gold from $Au^{3+}$ to $Au^{+}$ [22]. It is crucial that the reduction agent is weak, which means that only $Au^{+}$ is generated. Ascorbic acid is only capable of weak reduction during low pH, which is the case since HCl is added before the ascorbic acid in the growth solution. $Au^{+}$ is then only present during the addition of the seed solution and further nucleation is therefore prevented, since no $Au^{0}$ is present together with $Au^{3+}$. The reduction of $Au^{+}$ then occurs at the surface of the seeds which cause the seeds to grow, with a final outcome of gold nanorods.

$AgNO_3$ is another additive to the growth solution but the contribution of the silver ions to the synthesis is still not fully validated [22]. There are different theories why the silver ions influence the geometry of the gold nanoparticles and ease the formation of the cylindric shape, for instance by interacting with CTAB during the growth of the nanorods.

### 2.3.4 Electrostatic Surface Assembly

The gold nanorod-functionalisation of the glass substrates utilises the electrostatic interaction between the glass and the gold nanorods. To enable self assembly of the gold nanorods the glass is treated with $HNO_3$ (65-67%), with a purpose of cleaning. The concentrated acid has the properties to remove contamination upon the glass surface, for instance carbon-containing substances, $Ca^{2+}$, $Na^{+}$ and $Si^{4+}$ [23]. The surface is also left with negatively charged OH-groups which results in an electrostatic attraction between the nanorods and the glass. The attraction occurs because the CTAB capping the gold nanorods creates a positive surface charge [22]. The electrostatic interaction therefore immobilise the gold nanorods upon the surface of the glass, which is illustrated in figure 2.3. The acid treated substrates only need to be immersed in a dispersion of gold nanorods for the spontaneous assembly to occur.

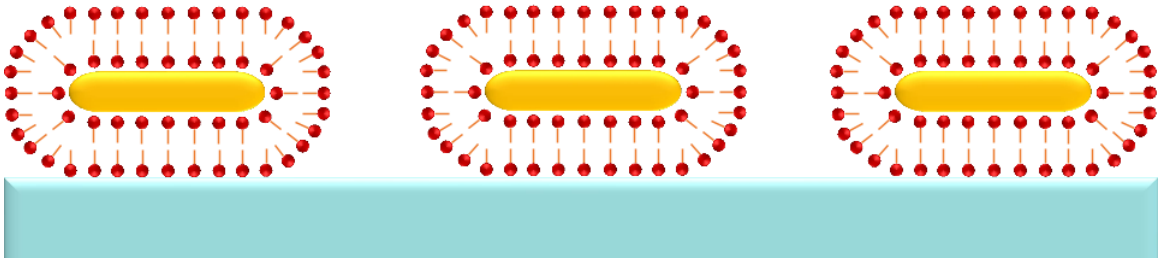

**Figure 2.3:** Gold nanorods electrostatically immobilised upon the glass surface. The elliptic shapes represent the gold nanorods, CTAB then capping the gold nanorods in a bilayer and the blue area illustrates the glass.

## 2.4 Combination of Antibiotics and Photothermal Gold Nanorods

The interest of nanoparticles in biomedical applications has only increased over the years. Existing studies have considered combining nanoparticles and antibiotics in different ways to find new ways of therapeutic treatment [24–27].

The synergism between antibiotics and heat has been proven by earlier research [3–6]. These studies implicate that the combination of heat and antibiotics more effectively eradicate bacteria compared to therapeutic treatment with the two methods apart. Where for instance one study concerns the combination of heat, originating from gold nanoparticles, and antibiotics in microneedle patches against skin infections [3].

The combination of photothermal gold nanorods exposed to NIR-light and antibiotics is therefore a promising alternative to decrease the usage of antibiotics and more effectively treat implant-associated infections. The combination of nanoparticles and antibiotics is also a field of much importance and where new discoveries are constantly taking place. Despite this, no extended research has yet been carried out regarding the combination of unfunctionalised photothermal gold nanorods immobilised on a surface together with antibiotics. The gold nanorods are supposed to be immobilised upon the implant surface meanwhile the antibiotics are present in solution. When exposed to NIR-light a simultaneous antimicrobial effect from the photothermal gold nanorods and from the antibiotics could more effectively eradicate the pathogen causing implant-associated infections. If a synergistic effect occurs this therapeutic method may be an alternative to decrease the usage of antibiotics.

## 2.5 Minimum Inhibitory Concentration (MIC)

The minimum inhibitory concentration (MIC) is the minimal concentration of an antimicrobial agent required to visually inhibit the growth of a certain bacterium [28]. The MIC declares the resilience of the bacteria towards a certain drug and can also determine the activity of newly developed antimicrobial agents. The two most

common techniques for evaluation are the agar dilution and broth dilution strategy, utilising standardised conditions. Agar dilution utilises the incorporation of different concentrations of antimicrobial agents into the nutrient agar medium. Meanwhile the broth dilution is a technique where a standardised amount of bacteria is mixed in liquid growth medium with geometrically increasing concentration of antimicrobial substance, often performed in 96-well plate [28]. After a certain incubation time is presence of turbidity a sign of bacterial growth meanwhile a visually transparent well indicate no bacterial growth. The well with the lowest concentration of antimicrobial agent that appear transparent is therefore determined as the MIC.

# 3
# Methodology

## 3.1 Materials

For the cleaning of glassware with basicpiranha were ammonia (28%, AnalaR NORMAPUR® analytical reagent, liquid, VWR chemicals), hydrogen peroxide (100 volumes >30% w/v, liquid, Fisher Scientific) and Milli-Q water (Millipore Q-Gard® 1) required. During the seed-mediated gold nanorod synthesis were gold(III) chloride trihydrate (≥99.9% trace metals basis, crystals and lumps, Sigma-Aldrich), Hexadecyltrimethylammonium bromide (≥98%, solids, Sigma-Aldrich), Sodium borohydride (99%, *ReagentPlus*®), powder, Sigma-Aldric, hydrochloric acid (≥37%, liquid, Sigma-Aldrich), silver nitrate (99.9999% trace metal basis, solid crystalline, Sigma-Aldrich), L-ascorbic acid (≥98%, crystalline, Sigma-Aldrich) and Milli-Q water (Millipore Q-Gard® 1) utilized. For the gold nanorod-functionalisation of glass substrates were ethanol (95%, liquid, Solveco), ethanol (99.5%, liquid, Solveco), nitric acid (65.0-67.0%, liquid, Sigma-Aldrich) and Milli-Q water (Millipore Q-Gard® 1). The gold nanorods were immobilised upon microscope slides (plain microscope slides,25·1·75 mm, Epredia$^{TM}$). For the *In-Vitro* studies were phosphate buffered saline (Sigma-Aldrich), brain heart infusion agar (powder, Millipore), tryptic soy broth (Nutriselect® Plus, powder, Millipore), cation-adjusted Mueller Hinton broth (Nutriselect® Plus, powder, Millipore) and Vancomycin hydrochloride (Pharmaceutical Secondary Standard; Certified Reference Material, neat, Supelco) used.

## 3.2 Basicpiranha Cleaning

All glassware used during procedures involving gold nanorods or during the nanorod synthesis was cleaned with basicpiranha. The mixture utilised had the ratio 4:1:1 of Milli-Q water, $NH_3$ and $H_2O_2$ and were added to all glassware. Milli-Q water and $NH_3$ were heated to 30 °C followed by addition of $H_2O_2$ and further heating to around 75 °C. The mixture was left for 15 minutes before switching of the heating plate and rinsing all glassware thoroughly with Milli-Q water.

## 3.3 Synthesis and Purification of Gold Nanorods

The performed synthesis, called a seed-mediated synthesis, was adapted from the described procedure in *A "Tips and Tricks" Practical Guide to the Synthesis of Gold Nanorods* [22].

### 3.3.1 Seed Solution

Firstly was a water bath prepared with a temperature of around 30 °C, where both seed and growth solution were stationed during the synthesis. 25 $\mu$l $HAuCl_4$ (50 mM) was added to 4.7 ml of CTAB (0.1 M) which was then slowly stirred for about 10 minutes, until no remaining turbidity. Thereafter, 300 $\mu$l of a freshly prepared solution of $NaBH_4$ (10 mM) was added during vigorous stirring (>1400 rpm). After 10-20 s was the solution again mildly stirred (400 rpm). The light brown solution was left for 30-45 minutes before use.

### 3.3.2 Growth Solution

The following procedure was performed in a water bath at around 30 °C. 1140 $\mu$l of HCl (1 M) and 600 $\mu$l of $HAuCl_4$ (50 mM) was added to 60 ml of CTAB (0.1 M) which was stirred for 10 minutes, the pH of the solution should be around 1.5. Thereafter was 720 $\mu$l of $AgNO_3$ (10 mM) added to the mixture and the solution was then stirred again for a few minutes. Subsequently was 600 $\mu$l of ascorbic acid (100 mM) added and the mixture was stirred for a few minutes once more, which should result in a colourless solution. Finally was 144 $\mu$l of the seed solution added to the growth solution and the solution was then thoroughly swirled. The mixture was then left undisturbed for 2 hours in the water bath.

### 3.3.3 Purification

For the purification of gold nanorods was a Thermo Heraeus Megafuge 16 R centrifuge utilised. The centrifuge was preheated to 28 °C and thereafter was the synthesis mixture centrifuged at 1900 G for 30 min followed by two centrifugations at 1800 G for 35 min. After the two first centrifugations was as much supernatant as possible removed without disturbing the pellet of gold nanorods. Subsequently was Milli-Q water added and the pellet was redispersed. The third centrifugation was succeeded by pipetting away 600 $\mu$l of the gold nanorod pellet and dispersing in 4.4 ml Milli-Q water, resulting in a concentration around 3 nM. The concentration has theoretically been calculated in Appendix A.1.

## 3.4 Preparation of Gold Nanorod-Functionalised Glass

The glass substrates were firstly rinsed with EtOH (95%) and subsequently washed thoroughly with Milli-Q water. The substrates were exposed to $N_2$ gas until totally dry and then placed in a clean petri dish. They were then covered with $HNO_3$ (65-67%) and left for around 17-18h. After the acid-treatment were the pieces of glass removed from the acid and placed in another clean petri dish containing Milli-Q water, left meanwhile preparing dispersion of gold nanorods.

A suitable dilution of the dispersion of nanorods, absorbance of 0.5-0.6 at 400 nm, was prepared. 600 $\mu$l of the solution was then added to each well in a well plate. The

glass substrates were removed from the petri dish and rinsed with Milli-Q water as well as shaken to remove excess water. While still wet was each substrate immersed into a well containing gold nanorod dispersion. They were then left between 2-4 h, for the gold nanorods to surface assemble. The gold nanorod dispersion was thereafter gradually removed by exchange with Milli-Q water until the solution turned colorless. The glass substrates were removed from the well plate, immersed into EtOH (99.5%) for a few seconds and then placed on a clean paper towel to air dry.

## 3.5 UV-Ozone Sterilisation

Before performing *In-Vitro* studies upon the gold nanorod-functionalised glass substrates were they sterilised to free them from foreign microorganisms and to remove the toxic CTAB encapsulating the nanorods. The substrates were placed on a sheet of aluminium foil and thereafter put in an UV-Ozone oven for 5 min. The substrates were then removed from the oven and directly transferred to a sterile petri dish, where left around 1-2 h before use.

## 3.6 *In-Vitro* Studies

In this section is the methodology regarding the *In-Vitro* studies presented. Firstly was the antimicrobial activity evaluated separately for the gold nanorods exposed to NIR-light and Vancomycin. Thereafter was the antimicrobial activity determined for both entities combined.

### 3.6.1 Photothermal Elimination

This methodology describes how the antimicrobial activity of the photothermal nanorods was determined for two differents systems; the gold nanorods irradiated covered with a thin liquid film and immersed in liquid.

The afternoon before performing the experiments was *S. aureus CCUG 10778* plated on brain heart infusion agar and incubated 18-24 h at 37 °C. One or several colonies were inoculated in 4 ml tryptic soy broth (TSB) and incubated at 37 °C until reaching $1{\cdot}10^9$ CFU/ml. When reaching $1{\cdot}10^9$ CFU/ml was the suspension diluted to $2{\cdot}10^8$ CFU/ml. The gold nanorod-functionalised substrates, sterilised as in section 3.5, were immersed into 400 $\mu$l of phosphate buffered saline (PBS) in a 24-well plate before addition of 600 $\mu$l diluted bacterial suspension to each well. The final bacterial concentration then became $1.2{\cdot}10^8$ CFU/ml for each well. The glass substrates were incubated in the bacterial suspension for 3 h at 37 °C.

Past incubation were all substrates immersed into a well with 2 ml PBS in a 24-well plate. 1.6 ml was then removed and 600 $\mu$l fresh PBS added, resulting in a total volume of 1 ml. If the substrates were to be irradiated immersed in liquid were they exposed to NIR-light in the well together with PBS. Thereafter the PBS

was removed, the substrate moved to a microscope slide and stained with 10 $\mu$l LIVE/DEAD$^{TM}$ *Bac*Light$^{TM}$ stain and topped with a cover glass. If the substrates were to be irradiated while covered with a thin liquid film was the 1 ml PBS removed and the substrates were moved to microscope slides. They were covered with 10 $\mu$l LIVE/DEAD$^{TM}$ *Bac*Light$^{TM}$ stain followed by addition of a cover glass. The substrates were thereafter exposed to NIR-light through the cover glass. The laser utilised to irradiate the samples was a diode laser at 808 nm by the manufacturer BWT Bejing. After NIR irradiation all samples were analysed with fluorescence microscopy.

### 3.6.2 Determination of Minimum Inhibitory Concentration (MIC)

The procedures for the MIC determination are presented in this section. Firstly were MIC determinations performed on planktonic bacteria. The MIC for planktonic bacteria was thereafter used as a starting point to determine the MIC for surface grown bacteria on gold nanorod-functionalised substrates.

#### 3.6.2.1 Planktonic Bacteria

MIC determinations with vancomycin was performed to evaluate the bacteria's, *S. aureus CCUG 10778*, susceptibility towards the antibiotic agent, in a planktonic state. The broth dilution methodology was implemented, adapted from *Agar and broth dilution to determine the minimum inhibitory concentration (MIC) of antimicrobial substances* [28].

The afternoon before performing the MIC determination was *S. aureus CCUG 10778* plated and incubated as in section 3.6.1, and stored in 4 °C until use. One or several colonies were dispersed and incubated as in section 3.6.1, until reaching $1{\cdot}10^9$ CFU/ml. The bacterial suspension was thereafter diluted to $1{\cdot}10^6$ CFU/ml.

10 different concentrations of vancomycin was prepared with the final concentrations 32, 16, 8, 4, 2, 1, 0.5, 0.25, 0.125 and 0.0626 mg/l in a 48-well plate, using cation-adjusted Mueller-Hinton Broth (CAMHB). Bacteria were also added to each well resulting in a final concentration of $5{\cdot}10^5$ CFU/ml. One growth control with only CAMHB and bacteria with a final concentration of $5{\cdot}10^5$ CFU/ml was also prepared, to evaluate the growth of bacterial cells without presence of vancomycin. One sterility control was also prepared with only CAMHB, to analyse potential bacterial contamination of the liquid medium. The 48-well plate with the prepared solutions was thereafter incubated for 16-20 h. The following day was the MIC visually determined.

#### 3.6.2.2 Surface Grown Bacteria

MIC determinations on bacteria cultivated on gold nanorod-functionalised surfaces were performed. The MIC for surface grown bacteria is very relevant to evaluate since bacteria causing implant-associated infections are cultivated on a surface. It

is therefore of high importance to conclude surface grown bacteria's susceptibility towards antibiotics.

The afternoon before performing the test was *S. aureus CCUG 10778* plated and incubated as in section 3.6.1. One or several colonies was dispersed and incubated as in section 3.6.1, until reaching $1{\cdot}10^9$ CFU/ml. The bacterial suspension was thereafter diluted and added to PBS as in section 3.6.1, with substrates serilised as described in section 3.5. The glass substrates were then incubated with bacteria for 3 h at 37 °C.

4 different concentrations of vancomycin was prepared with the final concentrations of 1, 2, 3, and 4 mg/l in a 24-well plate, using CAMHB. After incubating for 3 h were the surfaces immersed into 2 ml PBS followed by immersion into the antibiotic solutions. One control surface was also prepared by immersion in only CAMHB, to control the growth without presence of vancomycin. Thereafter were the substrates incubated for 18 h.

The next morning was the liquid in each well removed and the substrates were transferred to microscope slides. Every surface was covered with 10 $\mu$l LIVE/DEAD™ *Bac*Light™ stain and topped with a cover glass. The samples were then analysed with fluorescence microscopy.

### 3.6.3 Combination of Photothermal Elimination and Antibiotics

The antimicrobial activity of the combination of photothermal gold nanorods exposed to NIR-light and vancomycin could now be determined, after evaluating the antimicrobial activity of the two entities separately.

The afternoon before performing the experiments was *S. aureus CCUG 10778* plated and incubated as described in section 3.6.1. One or several colonies were dispersed and incubated as in section 3.6.1, until reaching $1{\cdot}10^9$ CFU/ml. The bacterial suspension was thereafter diluted and added to PBS as stated in section 3.6.1, with substrates sterilised as in section 3.5. The substrates were then incubated in 3 h at 37 °C.

After incubation in 3 h were the substrates immersed into 2 ml PBS followed by immersion in a 3 mg/l vancomycin solution. Certain substrates were thereafter irradiated with NIR-light while immersed liquid before incubation in 18 h. Control surfaces were prepared as described in section 3.6.2.2.

The next morning were the gold nanorod-functionalised substrates prepared as in section 3.6.2.2 before analysed with fluorescence microscopy.

## 3.7 Characterisation and Analytical Techniques

This section present the characterisation instruments implemented during the study and the instruments' intended use.

### 3.7.1 UV-Vis-NIR Spectroscopy

UV-Vis-NIR spectroscopy classify as an absorption spectroscopy technique which considers light in the ultraviolet, visible, and near-infrared region [29]. The technique is conducted by irradiating a sample with light and determine the amount of light absorbed by the sample, by comparing the transmitted light with the incoming light [30]. Absorbance generally quantify the light absorbed and is defined as in equation 3.1 below. Where A is the absorbance, $P_0$ is the incoming light and P is the transmitted light after passing through the sample.

$$A = log(\frac{P_0}{P}) \tag{3.1}$$

For this project were the analyses performed by a UV-Vis-NIR spectrometer of model OneC by the manufacturer Nanodrop for the wavelengths 300-800 nm. For the wavelengths 300-1000 nm was the spectrometer of model 8453 by the manufacturer Hewlett Packard utilised. UV-Vis-NIR spectroscopy was conducted to characterise the optical properties of the synthesised gold nanoparticles by locating the surface localised plasmon resonance bands. The technique was also implemented to analyse the concentration of gold nanorods after purification, since the concentration of gold nanorods can be correlated to the absorbance at 400 nm [22]. Additionally, UV-Vis-NIR spectrometry was performed on gold nanorod-funtionalised glass substrates immersed in Milli-Q water to evaluate if gold nanorods had surface assembled on the surfaces and if their photothermal properties was preserved after functionalisation.

### 3.7.2 Scanning-Electron Microscopy

A scanning-electron microscope (SEM) is a type of electron microscope which exposes a material's surface to high-energy electrons in the form of a very focused beam, which is scanned across the surface in vaccum [31]. The primary high-energy electrons interact with the specimen which generate signals, e.g secondary electrons, back-scattered electrons, X-rays, etc. The different electrons and X-rays generated contains different information and can for instance give knowledge about topography, morphology, composition and crystallographic information [31]. The microscope can also compose detailed images of the sample surface with high quality and resolution. The images are composed of information from secondary electrons and back-scattered electrons [32]. Secondary electrons are generated through inelastic interactions between the electron beam and the sample. The secondary electrons contain information regarding topography and morphology. Back-scattered electrons are generated through elastic interactions between the electron beam and the sample. The back-scattered electrons contain information related to the composition of the sample. The electrons yield contrast between light (eletron-dense) and

dark (electron-poor) areas of the sample surface.

During this study was a SEM of the model Ultra 55 LEO with a field emission gun by the manufacturer Zeiss implemented to analyse the gold nanorods, with an acceleration voltage of 2.5 kV. The analyses were performed on the gold nanorod-functionalised glass substrates and the SEM micrographs could thereafter be evaluated by image analysis, in *ImageJ*, to determine the geometry of the nanorods as well as the surface coverage of the gold nanorod-functionalised substrates.

### 3.7.3 Fluorescence Microscopy

Fluorescence microscopy is a type of optical microscopy where a light source is utilised to emit certain wavelengths to make the molecules fluoresce, to create an image [33]. Fluorophores, which are molecules making a specimen fluoresce, absorb light at one wavelength and emit light at a lower wavelength. The change in wavelength between the absorbed and emitted light increase the contrast of the composed image, since only the emitted light is detected against the dark background. A specimen can only fluoresce if it contains fluorophores which can occur naturally or by labelling.

Fluorescence microscopy has been implemented during the *In-Vitro* studies to determine the amount of live and dead bacteria on gold nanorod-functionalised glass substrates. The microscope utilised was an Axio Imager Z2m from the manufacturer Zeiss with an accompanying high-pressure mercury vapor arc-discharge (HBO) lamp as light source. The bacteria was analysed with 40x magnification succeeded by fluorescent staining with LIVE/DEAD$^{TM}$ *Bac*Light$^{TM}$. The stain decide the amount of live and dead bacteria depending on the membrane integrity by SYTO 9 and propidium iodide [34]. SYTO 9 can penetrate all cell membranes meanwhile propidium iodide only permeate cells with disrupted cell membranes. The live bacteria are stained with SYTO9 and will appear green, while dead bacteria with damaged membranes are stained by both SYTO9 and propidium iodide and will appear red.

# 4

# Results & Discussion

## 4.1 Synthesis of Gold Nanorods

This section present the properties of the synthesised gold nanorods. The nanorods were produced by a wet chemistry procedure and thereafter characterised by UV-Vis-NIR spectroscopy and SEM. Firstly are the plasmonic properties of the nanorods introduced and thereafter the rods' geometry.

### 4.1.1 Localised Surface Plasmon Resonance Spectrum

The synthesised nanoparticles' plasmonic properties were determined by UV-Vis-NIR spectroscopy. Figure 4.1 visualise a localised surface plasmon resonance spectrum for a batch of dispersed gold nanorods with a transverse absorption band around 520 nm and a longitudinal absorption band around 850 nm. The presence of two absorption bands and their distinct separation indicates that a majority of gold nanorods have been synthesised. The height relation between the peaks are also characteristic plasmonic behaviour of gold nanorods which indicates that no large amount of gold nanoparticles with other geometries are present, the absorbance at 500-600 nm would in that case be higher.

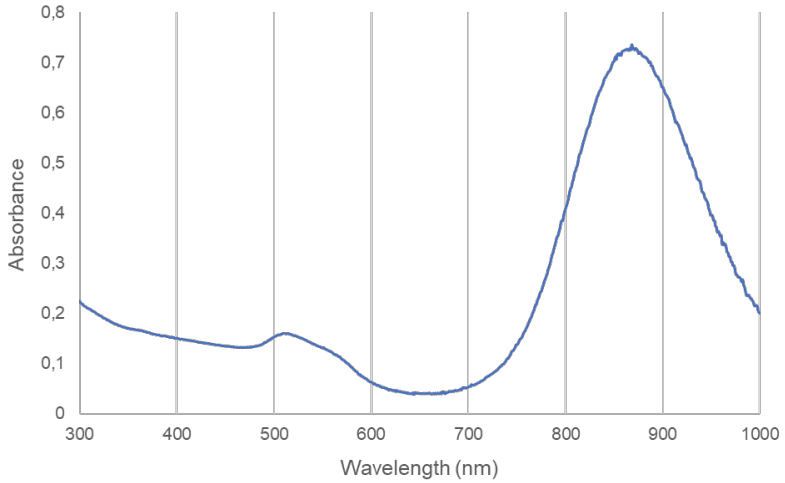


**Figure 4.1:** Localised surface plasmon resonance spectrum of gold nanorods dispersed in Milli-Q water.

The longitudinal absorption band at 850 nm for the synthesised nanorods is located

in the "biological-window". Declaring that the characteristics of the gold nanorods is suitable for their aimed application. The light absorption is also applicable for laser exposure at 808 nm, which will occur during the *In-Vitro* studies.

### 4.1.2 Geometry of Gold Nanorods

The dimensions of the nanorods were determined by performing image analysis of SEM micrographs in *ImageJ*. Width, length and aspect ratio were determined, which are presented in table 4.1. The average length of the nanorods was 64.0 nm, average width was 20.6 nm and the average aspect ratio (length/width) was 3.1 nm. All three parameters were calculated by analysing 2560 nanorods, which were projected with an rectangular area.

**Table 4.1:** Shows the dimensions of the synthesised gold nanorods, expressed as averages with standard deviations. AuNR is an abbreviation for gold nanorods.

| | Average Dimensions of AuNR |
|---|---|
| Length (nm) | 64.0 ± 8.2 |
| Width (nm) | 20.6 ± 3.8 |
| Aspect Ratio | 3.1 ± 0.58 |

## 4.2 Gold-Nanorod Functionalised Glass Substrates

This section present the characteristics of the gold nanorod-functionalised glass substrates. The substrates were functionalised after acid-treatment by immersion in gold nanorod dispersions, succeeded by characterisation with SEM and UV-Vis-NIR spectroscopy. Initially are SEM micrographs presented visualising the functionalised surfaces followed by the surface coverage and the plasmonic properties of the immobilised gold nanorods. The substrates used during this study were square microscope slides with an area of 1 $cm^2$.

### 4.2.1 SEM Micrographs

SEM was performed upon the gold nanorod-functionalised glass substrates to enable evaluation of the self assembly of gold nanorods. Figure 4.2 shows gold nanorod-functionalised glass with a magnification of 50 000x. The micrograph shows no presence of larger clusters, implicating that the nanorods' photothermal properties should still remain even though immobilised on a surface, which is desired for the aimed application. Because aggregation of gold nanorods results in plasmon coupling and change of plasmonic properties. Although the nanorods are evenly distributed on the glass substrates are parts of the plasmonic properties changed since the nanorods are forced closer to each other on the surface than in dispersion.

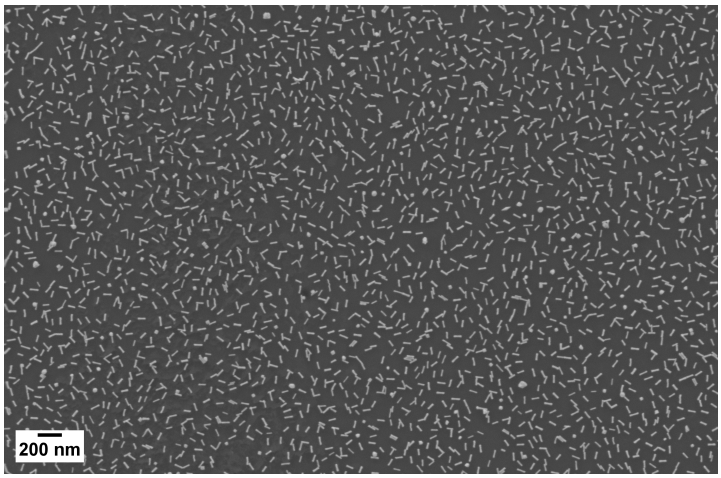


**Figure 4.2:** SEM micrograph of gold nanorod-functionalised glass with a magnification of 50 000x.

### 4.2.2 Surface Coverage

The surface coverage was determined by analysing representative SEM micrographs in *ImageJ*, where the gold nanorods were projected with a rectangular area. The surface coverage was 12.6% for the gold nanorod-functionalised substrates which equals 96 nanorods/$\mu$m$^2$. Table 4.2 presents the surface coverage of gold nanorod-functionalised glass substrates.

**Table 4.2:** Shows average surface coverage of gold nanorod-functionalised glass substrates with standard deviations.

| Surface Coverage (%) | Surface Coverage (nanorods/$\mu$m$^2$) |
|---|---|
| 12.6 $\pm$ 1.3 | 96 $\pm$ 10 |

### 4.2.3 Localised Surface Plasmon Resonance Spectrum

The immobilised nanorods' plasmonic properties were investigated by UV-Vis-NIR spectroscopy. Figure 4.3 shows a localised surface plasmon resonance spectrum of a gold nanorod-functionalised substrate, immersed in Milli-Q water, with a transverse absorption band around 520 nm and a longitudinal absorption band around 820 nm. Both absorption peaks are lower in intensity in figure 4.3 compared to figure 4.1 because of the lower concentration of nanorods on the glass surfaces compared to in dispersion. The peaks are also broader, especially the longitudinal absorption band. The peak broadening is probably due to the rods close fixation to one another on the glass, resulting in plasmon coupling. The plasmon coupling change the plasmonic properties of the nanorods and therefore change the peaks appearance.

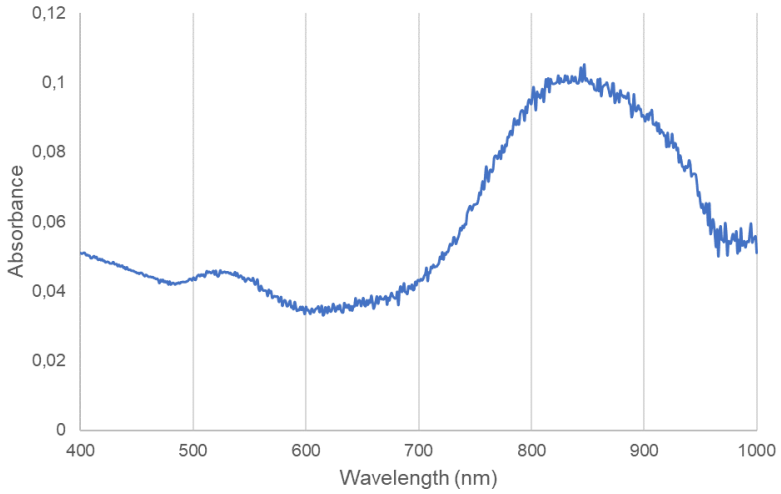


**Figure 4.3:** Localised surface plasmon resonance spectrum of gold nanorod-functionalised glass substrate immersed in Milli-Q water.

Figure 4.3 clearly states that the gold nanorods still possess the desired plasmonic properties, because of the similar characteristics between figure 4.3 and figure 4.1. The gold nanorod-functionalised substrates are therefore suitable for the aimed application since the immibilised gold nanorods have similar behaviour as gold nanorods in dispersion.

## 4.3 *In-Vitro* Studies

*In-Vitro* studies were performed to evaluate the antimicrobial activity of photothermal gold nanorods exposed to NIR-light and vancomycin separately as well as in combination. Firstly is the antimicrobial effect of the gold nanorods exposed to NIR-light presented. Thereafter is the antimicrobial activity of the antibiotics on both planktonic and surface grown bacteria introduced. Lastly, is the antimicrobial activity of the two entities combined stated.

### 4.3.1 Photothermal Elimination

In this section is only the antimicrobial effect of the gold nanrods when irradiated with NIR-light evaluated, before combining the nanopartices with antibiotics. The antimicrobial activity was evaluated after irradiation of gold nanorod-functionalised substrates with cultivated bacteria. The activity was determined for two systems, one when the substrates was covered with a thin liquid film and the other when the substrates were immersed in liquid.

#### 4.3.1.1 Irradiation while Covered with Thin Liquid Film

For this system was the antimicrobial effect evaluated for the gold nanorods exposed to NIR-light when the bacteria were cultivated on the substrate surface for 3 h. Thereafter were the substrates covered with 10 $\mu$l LIVE/DEAD$^{TM}$ *Bac*Light$^{TM}$

stain before irradiation. After irradiation were the substrates analysed with fluorescence microscopy.

Figure 4.4 shows double channel fluorescence microscopy images of live and dead *S. aureus* on gold nanorod-functionalised substrates covered with a thin liquid film during irradiation. Figure 4.4a shows a substrate after irradiation with 24 W/cm$^2$ for 10 s (AuNR + NIR) and figure 4.4b shows a substrate without exposure to NIR-light (AuNR). The amount of live bacteria is represented by the green channel and the dead bacteria by the red channel, single channel images are shown in Appendix figure A.1. Figure 4.4 clearly states that an antimicrobial effect was achieved when the substrates were irradiated with 24 W/cm$^2$ for 10 s. Since there is a clear distinction between the amount of dead bacteria depending on whether the gold nanorod-functionalised substrates were exposed to NIR-light.

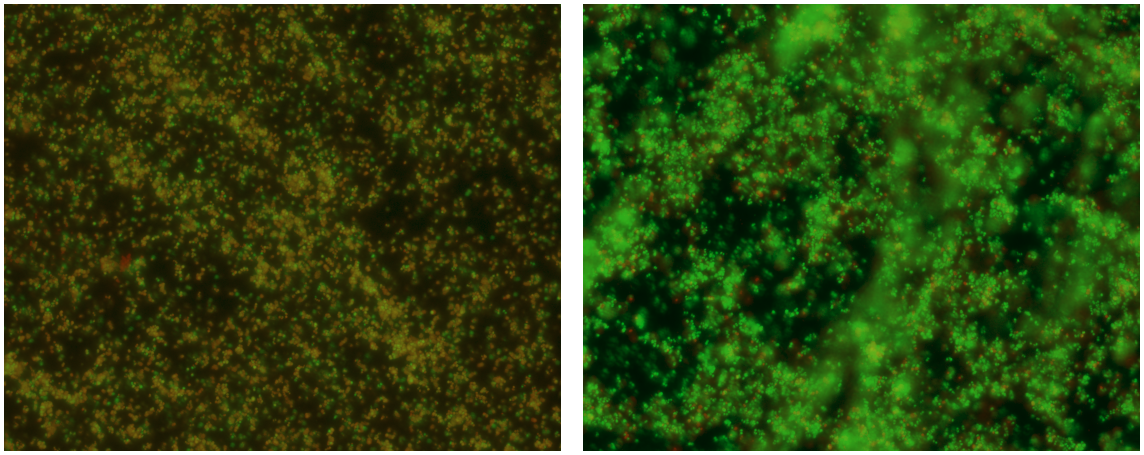

**(a)** NIR-light. **(b)** No NIR-light.

**Figure 4.4:** Microscope images of live and dead *S. aureus* on gold nanorod-functionalised glass covered by a thin liquid film during irradiation. (a) After irradiation with 24 W/cm$^2$ for 10 s and (b) with no NIR exposure.

By image analysis in *ImageJ* has an average percentage of dead bacteria been estimated for each sample group, by determining the amount of dead bacteria on all three replicates. The average percentage of dead bacteria for each sample group is shown in figure 4.5. The percentage of dead bacteria was calculated by dividing the amount dead bacteria on a substrate with the total amount bacteria on the same substrate and thereafter was an average calculated for each sample group. The average percentage of dead bacteria for AuNR was 7% and for AuNR + NIR 59%. A significant difference in the amount of dead bacteria was determined between the sample groups AuNR + NIR and AuNR when performing a t-test with a significance level of 1% (*). The results therefore show that an antimicrobial effect was achieved for the system.

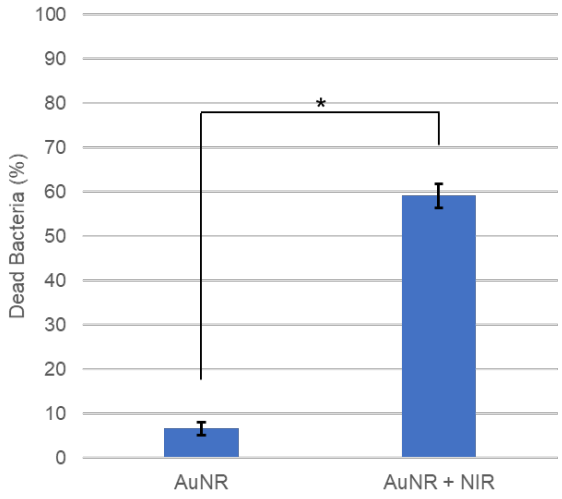


**Figure 4.5:** Visualise the percentage of dead bacteria on gold nanorod-functionalised glass covered with a thin liquid film. Which was calculated by dividing the amount dead bacteria on a substrate with the total amount bacteria on the same substrate. Showing one sample group without exposure to NIR-light (AuNR) and with exposure to 24 W/cm$^2$ for 10 s (AuNR + NIR). The two sample groups show a significant difference in the amount of dead bacteria with significance level of 1% (*).

The average percentage of dead bacteria for the sample groups presented in figure 4.5 are only rough estimations because of the manual thresholding of the images during analysis in *ImageJ*. The manual thresholding result in an increased source of error during the image analysis which needs to be concenrned when interpreting the results.

The gold nanorod-functionalised substrates demonstrate an antimicrobial activity for the irradiation parameters 24 W/cm$^2$ for 10 s. The source of the antimicrobial effect is most likely macroscopic heating of the thin liquid film with heat originating from the gold nanorods when exposed to NIR-light. The macroscopic heating can eliminate the bacteria by increase in temperature and evaporation of the thin film, which will cause the pathogen to dry. Which means that the bacteria are not eliminated by the heat transferred from the nanorods to the bacteria, caused by the contact between them. Macroscopic heating of the liquid is not suitable for clinical use, since it would indicate more or less boiling of surrounding tissue. The system is neither suitable for further evaluation in combination with antibiotics since the concentration of the thin liquid film cannot be controlled.

The results indicates that an antimicrobial effect can be achieved by macroscopic heating of a thin liquid film but also prove that the gold nanorods are photothermally active. Their photothermal properties give rise to the macroscopic heating of the liquid and cause the elimination of the pathogen.

#### 4.3.1.2 Irradiation while Immersed in Liquid

For this system was the antimicrobial effect evaluated of the gold nanorods exposed to NIR-light when the bacteria were cultivated on the substrate surfaces for 3 h and thereafter immersed into 1 ml PBS during irradiation. The PBS was removed and the substrates were stained with LIVE/DEAD™ *Bac*Light™ stain before analysed with fluorescence microscopy. This system was investigated to evaluate the antimicrobial activity of the gold nanorods exposed to NIR-light when the substrates are immersed in liquid but also since this system is easier in terms of evaluating a combined effect with antibiotics.

To compare with the antimicrobial activity of section 4.3.1.1 were the laser parameters 24 W/cm$^2$ for 10 s evaluated for this system as well. Figure 4.6 shows double channel fluorescence microscopy images of live and dead *S. aureus* on gold nanorod-functionalised glass substrates immersed in 1 ml PBS during irradiation. Figure 4.6a shows a substrate after irradiation with 24 W/cm$^2$ for 10 s (AuNR + NIR) and figure 4.6b shows a surface without exposure to NIR-light (AuNR). The amount of live bacteria is represented by the green channel and the dead bacteria by the red channel, single channel images are shown in Appendix figure A.2. Figure 4.6 shows no distinct difference in the amount of dead bacteria depending on whether the gold nanorod-fuctionalised substrates were exposed to NIR-light. No antimicrobial activity is therefore achieved for the laser parameters 24 W/cm$^2$ for 10 s when the substrates are irradiated while immersed in liquid.

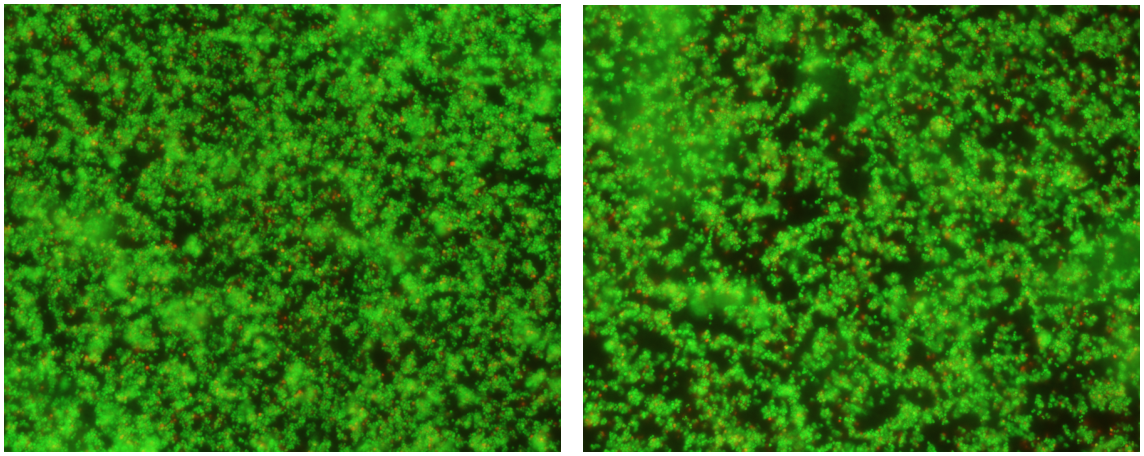

**(a)** NIR-light. **(b)** No NIR-light.

**Figure 4.6:** Microscope images of live and dead *S. aureus* on gold nanorod-functionalised glass immersed in liquid during irradiation. (a) After irradiation of 24 W/cm$^2$ for 10 s and (b) with no NIR exposure.

By image analysis in *ImageJ* has an average percentage of dead bacteria been estimated for each sample group, by determining the amount of dead bacteria on all three replicates. The average percentage of dead bacteria for each sample group is shown in figure 4.7. The average percentage of dead bacteria was estimated by dividing the amount dead bacteria on a substrate with the total amount of bacte-

ria on the same substrate and thereafter was an average calculated for each sample group. The average percentage of dead bacteria for AuNR was 10% and for AuNR + NIR 11%. No significant difference in the amount of dead bacteria was determined between the sample groups AuNR and AuNR + NIR when performing a t-test with a significance level of 1%.

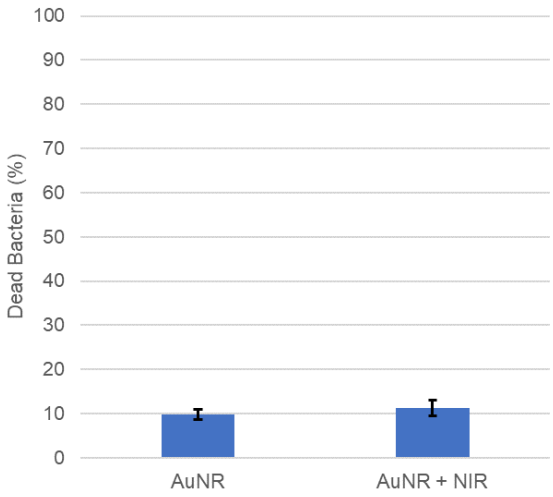


**Figure 4.7:** Shows the percentage of dead bacteria on gold nanorod-functionalised glass immersed in liquid. Which was calculated by dividing the amount dead bacteria on a substrate with the total amount bacteria on the same substrate. Showing one sample group without exposure to NIR-light (AuNR) and with exposure to 24 W/cm$^2$ for 10 s (AuNR + NIR) .

The average percentage of dead bacteria for the sample groups presented in figure 4.7 is only a rough estimation because of manual thresholding during image analysis, equal to section 4.3.1.1.

The gold nanorod functionalised substrates demonstrate no antimicrobial activity for the irradiation parameters 24 W/cm$^2$ for 10 s, compared to section 4.3.1.1. The two systems differ on many aspects which result in a variation in the antimicrobial activity of the gold nanorod-functionalised surfaces when exposed to NIR-light.

Immersion of the gold nanorod-functionalised substrates in 1 ml PBS during irradiation imply that no macroscopic heating occur. Which was validated by temperature measurements before and after irradiation with NIR-ligt, with an IR-thermometer. The average temperature increase was 1-2 °C. The bacteria would therefore not be eliminated by a macroscopic increase in temperature when irradiated with 24 W/cm$^2$ for 10 s. The bacteria would neither be eliminated by drying of the bacteria since the substrates are immersed in liquid The system therefore evaluates the antimicrobial activity of the photohermal heat originating from the gold nanorods and transeferred to the bacteria, not macroscopic heating of a thin liquid film.

One possible explanation why a similar antimicrobial activity could not be achieved between section 4.3.1.1 and 4.3.1.2 is because the larger volume of liquid may allow

detachment of pathogen from the surface during exposure to NIR-light, since there is a possibility that the bacteria sense the heat change of the surface. Resulting in that the antimicrobial activity may become less efficient since the heat development originating from the rods is very local [35]. The detached bacteria are then less affected by the heat emitted which prevents their elimination. The heat emitted from the photothermal gold nanorods could also be insufficient to eliminate *S. aureus* because of the small contact area between the bacteria and the rods. The spherical *S. aureus* has a diameter around 1 $\mu$m meanwhile the rods has an average length of 64 nm and an average width of 20.6 nm, meaning that the bacteria are much larger than the rods. The contact area between the larger spherical pathogen and a nanorod is therefore very small, since only a fraction of the projected area for the spherical bacteria will be attached to the substrate. The heat transferring from the nanorods to the bacteria may therefore not be enough to effectively eliminate the pathogen cultivated on the surface.

### 4.3.2 Determination of Minimum Inhibitory Concentration (MIC)

In this section the results from the determination of the minimum inhibitory concentration of vancomycin for *S. aureus* is presented. The MIC values were determined for two systems, one with planktonic bacteria and the other with bacteria cultivated on gold nanorod-functionalised glass substrates.

#### 4.3.2.1 Planktonic Bacteria

A standardised MIC determination on planktonic bacteria using the broth dilution methodology with vancomycin was repeated four times. The results achieved were that the MIC varied between 1 mg/l and 2 mg/l. These values agree with data from *The European Committee on Antimicrobial Susceptibility Testing* (EUCAST) regarding MIC for *S. aureus*.

The variations in MIC may occur because of alterations in optical density (OD) for the different bacterial suspensions used for the MIC determinations, since OD can be correlated to the amount of bacteria present in the suspension. The different amounts of bacteria present in the antibiotic solutions may have influenced the MIC for the tests. The growth of bacteria may also have varied resulting in different MIC, since growth also has responsibility for the amount of bacteria present in the antibiotic solutions.

#### 4.3.2.2 Surface Grown Bacteria

The MIC for bacteria cultivated on gold nanorod-functionalised surfaces was also determined. The reason is because the MIC of surface grown bacteria is more relevant for the study since surface grown bacteria cause implant-associated infections. It is therefore of importance to evaluate the surface grown bacteria's susceptibility

towards antibiotics, in this case vancomycin.

The MIC determination for surface grown bacteria was performed by cultivating bacteria on the gold nanorod-functionalised glass substrates for 3 h followed by immersion into antibiotic solutions. They where thereafter incubated for 18 h. After incubation was the liquid removed and the substrates were stained with LIVE/DEAD™ *Bac*Light™ stain and analysed with fluorescence microscopy.

Figure 4.8 shows double channel microscopy images of live and dead *S. aureus* on gold nanorod-functionalised substrates after incubation in different concentrations of vancomycin for 18 h. Figure 4.8a shows a substrate after incubation without vancomycin (0 mg/l), 4.8b in 1 mg/l vancomyin, 4.8c in 2 mg/l vancomycin, 4.8d 3 mg/l vancomycin and 4.8e in 4 mg/l vancomycin. The amount of live bacteria is represented by the green channel and the amount of dead bacteria by the red channel, single channel images are presented in Appendix in figure A.3. Figure 4.8 shows a similar behaviour between the bacterial growth for the concentrations 0 mg/l, 1 mg/l, 2 mg/l and 3 mg/l. The alteration in bacterial growth occurs when changing the concentration of vancomycin from 3 mg/l to 4 mg/l. The MIC therefore determined to be located at 4 mg/l.

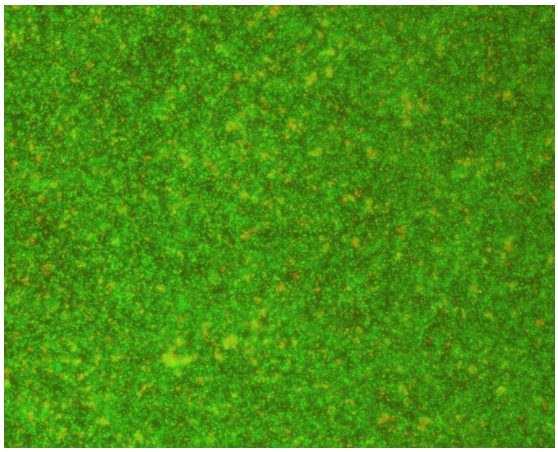

**(a)** 0 mg/l.

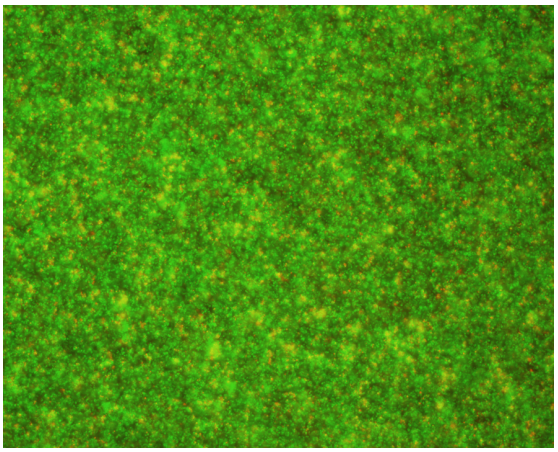

**(b)** 1 mg/l.

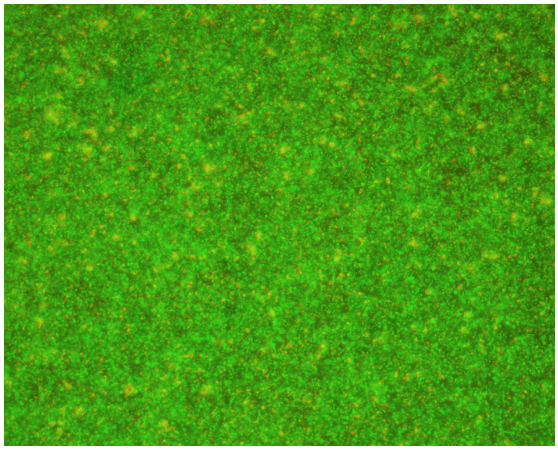

**(c)** 2 mg/l.

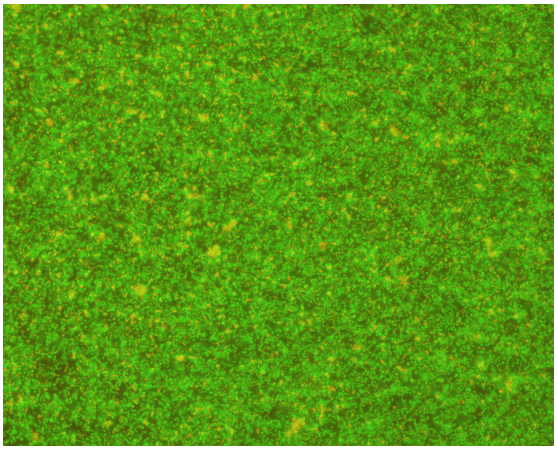

**(d)** 3 mg/l.

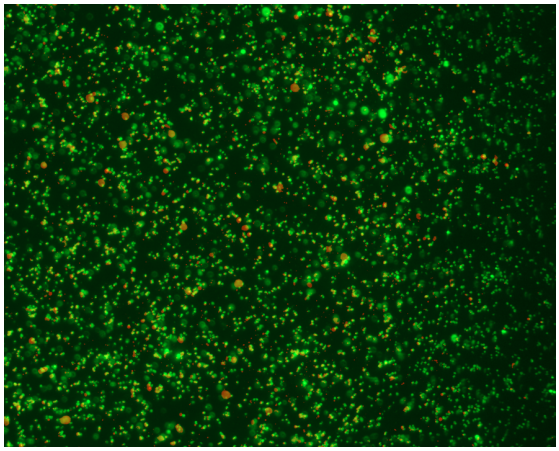

**(e)** 4 mg/l.

**Figure 4.8:** Microscope images of live and dead *S. aureus* on gold nanorod-functionalised glass after incubation in different concentrations of vancomycin for 18 h. (a) No vancomycin, (b) 1 mg/l vancomycin, (c) 2 mg/l, (d) 3 mg/l and (e) 4 mg/l.

By image analysis in *ImageJ* has an average percentage of live bacteria been estimated for each sample group, by determining the amount of live bacteria on all

three replicates. The average percentage of dead bacteria for each sample group is shown in figure 4.9. The average of live bacteria has been estimated because the essential difference after incubation in various concentrations of vancomycin is not the amount dead bacteria but instead the amount live bacteria cultivated on the substrates. The percentage live bacteria on each substrate was therefore estimated by dividing the amount of live bacteria on each substrate incubated in antibiotic solutions with the amount of live bacteria on a control substrate incubated without vancomycin and thereafter was an average determined for every sample group. The bacterial growth on the control substrate is therefore assumed to be 100 %.

Figure 4.9 shows that the average percentage of live bacteria for 0 mg/l vancomycin was 100%, for 1 mg/l vancomycin 102%, for 2 mg/l vancomycin 96%, for 3 mg/l vancomycin 99% and for 4 mg/l vancomycin 2%. A significant difference in the amount of live bacteria was determined between all other concentrations of vancomycin and 4 mg/l vancomycin when performing a t-test with a significance level of 1% (*). Figure 4.9 shows that the bacterial growth is unaffected when varying the concentration of vancomycin from 1 mg/l to 3 mg/l, which is also visible in figure 4.8. The drastic change in bacterial growth takes place when adjusting the concentration from 3 mg/l to 4 mg/l, where the bacterial growth goes from 99% to 2%. The results indicate that the concentration 4 mg/l of vancomycin is high enough to in a great extent disturb the growth of the bacterial cells when incubating the substrates for 18 h.

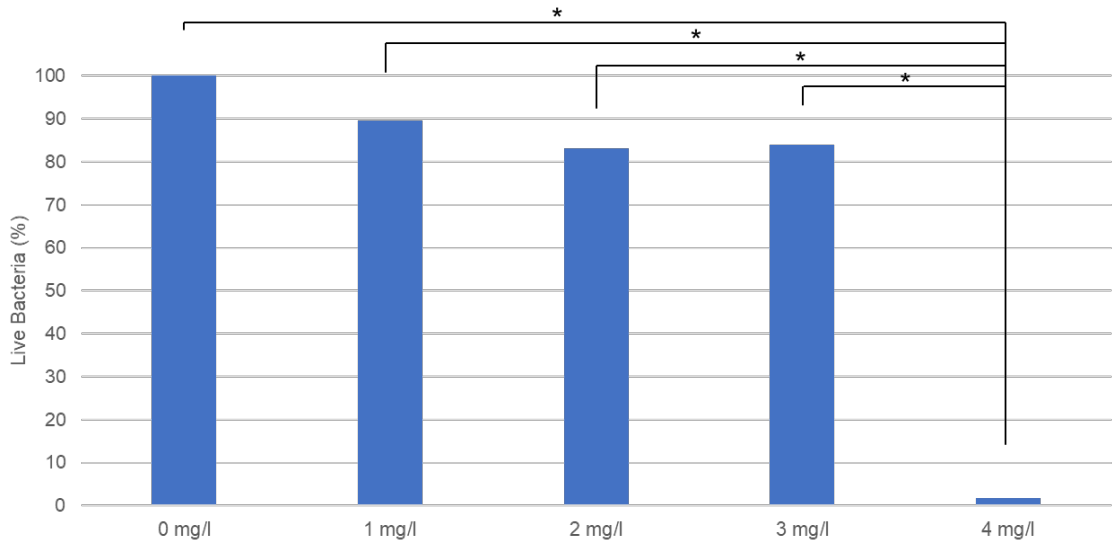


**Figure 4.9:** Visualise the percentage of live bacteria on gold nanorod-functionalised glass after incubation in vancomycin. Which was calculated by dividing the amount live bacteria on each substrate with the amount live bacteria on a control substrate (0 mg/l). Showing substrates incubated in following concentrations of vancomycin 0 mg/l, 1 mg/l, 2 mg/l, 3 mg/l and 4 mg/l for 18 h.

The results show that the MIC for surface grown bacteria is higher compared to planktonic bacteria. Which may be possible because the antibiotics cannot encounter the bacteria from all directions when cultivated on a surface which may

result in a decrease in the susceptibility towards antibiotics.

When evaluating data as in figure 4.9 can the growth of bacteria be higher for substrates incubated in concentrations of vancomycin lower than MIC compared to the control surface. This may occur because the amount of cultivated bacteria on the substrates can vary, when incubated in bacterial suspension for 3 h. When incubated in vancomycin with concentrations lower than MIC is the amount of antibiotic agent to low to disturb further growth of the bacteria and the growth can therefore become higher than for the control, like for sample group 1 mg/l. The average percentage of live bacteria cultivated on the gold nanorod-functionalised substrates are also rough estimations because of the manual thresholding of the images during image analysis, as in section 4.3.1.1.

### 4.3.3 Combination of Photothermal Elimination and Antibiotics

For this section is the antimicrobial activity of vancomycin combined with photothermal gold nanorods exposed to NIR-light evaluated. The concentration of vancomycin was set to 3 mg/l to evaluate if a possible synergy can increase the susceptibility of the pathogen towards antibiotics, which enables elimination of bacteria at a concentration lower then MIC for surface grown bacteria. The gold nanorod-functionalised substrates were irradiated after immersion in antibiotic solutions to determine if the photothermal heat originating from the gold nanorods can weaken the bacteria and make them more susceptible to antibiotics. Both the amount of live and dead bacteria were evaluated for each sample group in this section. Since the effects of a possible synergy for the combination of photothermal gold nanorods and vancomycin is unknown. A possible synergistic effect may either increase the amount of dead bacteria, as in section 3.6.1, or inhibit the bacterial growth, as in section 4.3.2.2.

For this system were the gold nanorod-functionalised substrates cultivated with bacteria for 3 h and immersed in 600 $\mu$l antibiotic solutions during irradiation, with 3 mg/l vancomycin. The substrates were irradiated with 3 W/cm$^2$ for 1 min and thereafter incubated for 18 h. After incubation was the liquid removed and the substrates were stained with LIVE/DEAD$^{TM}$ *Bac*Light$^{TM}$ stain followed by analysis with fluorescence microscopy.

Figure 4.10 shows double channel fluorescence microscopy images of live and dead *S. aureus* on gold nanorod-functionalised glass substrates after incubation for 18 h. Figure 4.10a shows a substrate after irriadiation with 3 W/cm$^2$ for 1 min and incubated without vancomycin (NIR), figure 4.10b shows a substrate after incubation in 3 mg/l vancomycin (Vanc) and figure 4.10c shows a substrate after exposure with 3 W/cm$^2$ for 1 min and incubated in 3 mg/l vancomycin (Vanc + NIR). The amount of live bacteria is represented by the green channel and the amount of dead bacteria by the red channel, single channel images are presented in Appendix figure A.4. Figure 4.10 shows no distinct difference in the amount of dead bacteria nor

bacterial growth for the substrates.

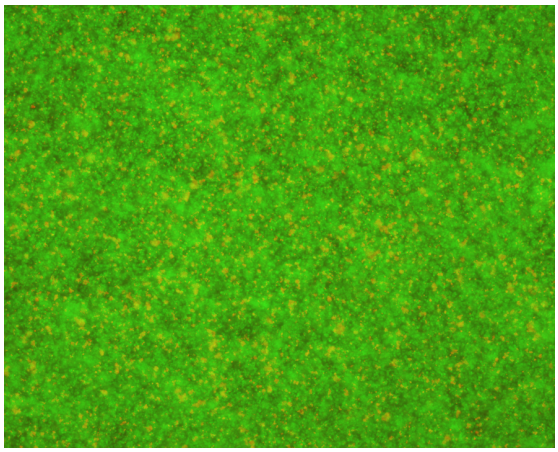

**(a)** NIR-light.

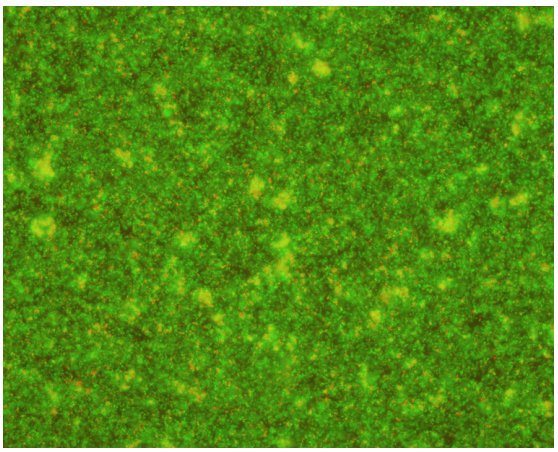

**(b)** Vancomycin.

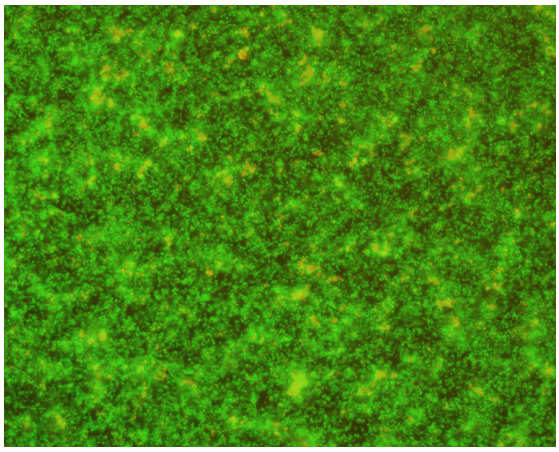

**(c)** NIR-light + Vancomycin.

**Figure 4.10:** Microscope images of live and dead *S. aureus* on gold nanorod-functionalised glass immersed in antibiotic solutions during irradiation and thereafter incubated for 18 h. (a) After irradiation with 3 W/cm$^2$ for 1 min and incubated without vancomycin, (b) after incubation in 3 mg/l vancomycin and (c) after irradiation with 3 W/cm$^2$ for 1 min and incubation in 3 mg/l vancomycin.

By image analysis in *ImageJ* has an average percentage of dead bacteria been estimated for each sample group, by determining the amount of dead bacteria on all three replicates. The average percentage of dead bacteria for each sample group is shown in figure 4.11. The percentage of dead bacteria was calculated by dividing the amount dead bacteria on a substrate with the total amount of bacteria on the same substrate and thereafter was an average calculated for each sample group. The average percentage of dead bacteria for NIR was 2%, for Vanc 3% and for NIR + Vanc 4 %. No significant difference in the percentage of dead bacteria was determined between the sample group NIR + Vanc and the two control groups Vanc and NIR when performing a t-test with a significance level of 1%. These findings indicate that no synergistic effect is present between the gold nanorods exposed to NIR-light and vancomycin for the laser parameters 3 W/cm$^2$ for 1 min and concentration 3

mg/l vancomycin with incubation for 18 h.

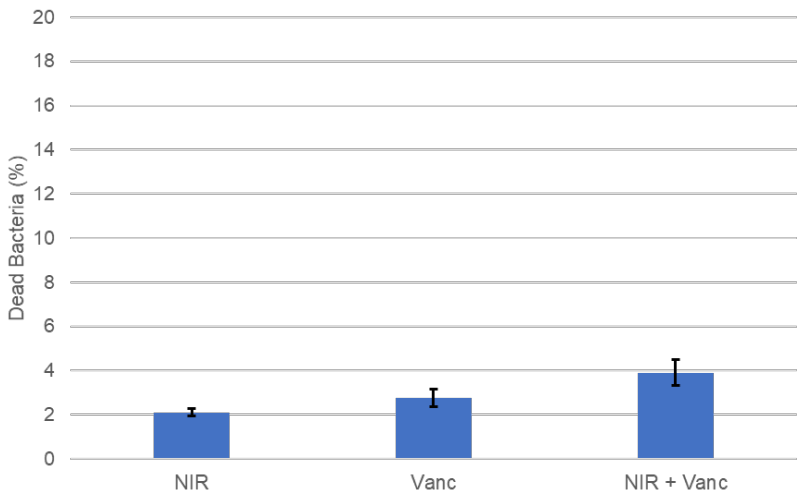


**Figure 4.11:** Visualise the percentage of dead bacteria adsorbed on gold nanorod-functionalised substrates. Which was calculated by dividing the amount dead bacteria on a substrate with the total amount bacteria on the same substrate. Showing substrates after irradation with 3 W/cm$^2$ for 1 min and incubated without Vancomycin for 18h (NIR), after incubated in 3 mg/l Vancomycin for 18 h (Vanc) and after irradiation with 3 W/cm$^2$ for 1 min and incubated in 3 mg/l Vancomycin for 18 h (NIR + Vanc).

By image analysis in *ImageJ* was also an average percentage of live bacteria estimated for each sample group, by determining the amount of live bacteria on all three replicates. The average percentage of live bacteria for each sample group are shown in figure 4.12. The average percentage of live bacteria was estimated by dividing the amount of live bacteria on a sample with the amount of live bacteria a control substrate (NIR) and thereafter was an average calculated for each sample group. The bacterial growth of sample group NIR is therefore assumed to be 100 % in figure 4.12. The percentage of live bacteria for each sample group was estimated since it is unknown if the combined effect of photothermal gold nanorods exposed to NIR-light and antibiotics increase the amount of dead bacteria, as in section 3.6.1, or inhibit the growth of bacteria, as in section 4.3.2.2.

Figure 4.12 shows that the average of live bacteria for sample group NIR is 100 %, for Vanc 82 % and for NIR + Vanc 81 %. No significant difference in the percentage of live bacteria was determined between the sample group NIR + Vanc and the two groups Vanc and NIR when performing a t-test with a significance level of 1%. These results further strengthen that no synergistic effect between the photothermal gold nanorods and vancomycin is achieved for the laser parameters 3 W/cm$^2$ for 1 min and a concentration of 3 mg/l vancomycin with incubation for 18 h.

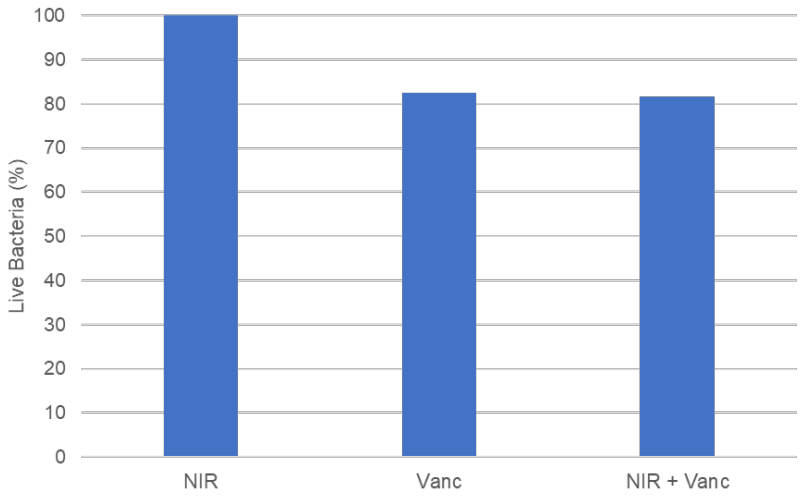


**Figure 4.12:** Visualises the percentage of live bacteria on gold nanorod-functionalised substrates. Which was calculated by dividing the amount of live bacteria on a sample with the amount live bacteria on a control substrate (NIR). Showing substrates after irradiation with 3 W/cm$^2$ for 1 min and incubated without Vancomycin for 18 h (NIR), after incubated in 3 mg/l Vancomycin for 18 h (Vanc) and after irradiation with 3 W/cm$^2$ for 1 min and incubated in 3 mg/l for 18 h (NIR + Vanc).

The average of amount live and dead bacteria for the substrates are only rough estimations because of the manual thresholding in *ImageJ* during image analysis, as mentioned in section 3.6.1.

The combination of photothermal gold nanorods exposed to the laser parameters 3 W/cm$^2$ for 1 min and incubation in 3 mg/l vancomycin for 18 h shows no indication of a synergistic effect. One possible explanation why a synergistic effect could not be achieved is the small contact area between the bacteria and gold nanorods, as introduced in section 4.3.1.2. The heat transferred from the nanorods to the bacteria may therefore be insufficient to create synergy between the antibiotics and the photothermal heat, since the synergy between heat and antibiotics often regards macroscopic heating [3–6]. The heat transferred from the rods may therefore not be enough to create a synergistic effect. This theory can be applied for his system since the volume of 600 $\mu$l liquid prevented macroscopic heating. Proved by temperature measurements before and after irradiation with NIR-light with an IR-thermometer. The average temperature increase was 1-2 °C.

# 5

# Conclusion & Future Studies

This thesis has evaluated the antimicrobial activity against *S.aurues* of photothermal gold nanorods exposed to NIR-light and of vancomycin, as well as combination of the two. Initially was gold nanorods successfully produced with an average length of 64 nm and an average width och 20.6 nm, which resulted in a longitudinal absorption band around 850 nm. The gold nanorods were surface assembled upon glass substrates by electrostatic interaction resulting in an average surface coverage of 12.6 %. The photothermal properties of the surface assembled nanorods could be proven preserved by performing UV-Vis-NIR spectroscopy on gold nanorod-functionalised substrates immersed in Milli-Q water.

*In-Vitro* studies were performed where the antimicrobial activity of the gold nanorods exposed to NIR-light and the antibiotics was evaluated separately, whereafter their combined effect was evaluated. An antimicrobial effect could be achieved when exposing the gold nanorod-functionalised substrates with cultivated bacteria to NIR-light when covered with a thin liquid film. The amount of dead bacteria was observed to be 59% upon irradiation with NIR-light of 24 W/cm$^2$ for 10 s meanwhile 7 % without irradiation. The gold nanorod-functionalised substrates were also immersed in PBS during irradiation with NIR-light. However, an antimicrobial effect could not be achieved by exposing the gold nanorod-functionalised substrates to NIR-light of 24 W/cm$^2$ for 10 s. The amount of dead bacteria was observed to 11% upon exposure to NIR-light and 10% without exposure.

The minimum inhibitory concentration for vancomycin and *S. aureus* was determined for both planktonic bacteria and bacteria cultivated on gold nanorod- functionalised surfaces. The MIC was located between 1-2 mg/l for planktonic bacteria and 4 mg/l for surface grown bacteria.

The gold nanorods exposed to NIR-light and vancomycin were combined to decide if a synergistic effect was present. No synergism could be noticed when the gold nanorod-functionalised substrates with cultivated bacteria was exposed to NIR-light of 3 W/cm$^2$ for 1 min and thereafter incubated in 3 mg/l vancomycin for 18 h. The percentage of dead bacteria when exposed to only NIR-light was 2% and only incubated in vancomycin 3%. The amount dead bacteria when irradiated with NIR-light and incubated in vancomycin was 4%. The percentage of live bacteria were also determind by assuming 100 % bacterial growth on the substrates only exposed to NIR-light and comparing with the remaining sample groups. The percentage of live bacteria when exposed to only NIR-light was therefore 100 % and only incubated in

vancomycin 82 %. The amount of live bacteria when irradiated with NIR-light and incubated in vancomycin was 81 %. The results indicate that no synergistic effect was achieved by combining photothermal gold nanorods and vancomycin.

Future studies are required to further evaluate the combination of photothermal heat emitted from gold nanorods and antibiotics, since this thesis only is a pilot study of the topic. More data needs to be generated concerning several laser parameters and concentrations of vancomycin before concluding whether a synergistic effect can be achieved. Experiments when irradiating the samples after incubation instead of before should also be performed to evaluate if a synergy can be observed. Refinements of the evaluation procedure is also essential to achieve more consistent and reliable results when studying the combination of the entities. Other quantification techniques should also be implemented as a complement to the image analysis of fluorescence microscopy images.

Future research is also necessary to study the interaction between the bacteria and the gold nanorods. To increase the understanding why an antimicrobial effect cannot be achieved when the gold nanorod-functionalised substrates with cultivated bacteria are exposed to NIR-light immersed in liquid, with and without vancomycin. It may be of interest to alter the geometry of the gold nanorods to increase the contact area between the rods and the bacteria, which may increase the antimicrobial activity. The contact area could also be increased by increasing the surface coverage of gold nanorods upon the glass substrates. Another topic to consider in future studies is to functionalise the nanorods to introduce a higher attraction between the bacteria and the rods to prevent a potential detachment of the pathogen from the surface when the temperature change, which may also increase the antimicrobial activity.

This study do not conclude that synergism cannot be achieved between photothermal heat emitted from the gold nanords and antibiotics. Only that more studies needs to be performed to solve the challenges regarding combining the two entities. Hopefully, resulting in an increase in the heat transferred from the gold nanorods to the bacteria, which may enable synergy between the photothermal heat and antibiotics.

# Bibliography


[1] Maria Pihl, Ellen Bruzell, and Martin Andersson. "Bacterial biofilm elimination using gold nanorod localised surface plasmon resonance generated heat". In: *Materials Science and Engineering: C* 80 (2017), pp. 54–58. DOI: https://doi.org/10.1016/j.msec.2017.05.067.

[2] Carla Renata Arciola, Davide Campoccia, and Lucio Montanaro. "Implant infections: adhesion, biofilm formation and immune evasion". In: *Nature Reviews Microbiology*. Oxford: Springer Nature, 2018, pp. 397–409. DOI: https://doi.org/10.1038/s41579-018-0019-y.

[3] Jill Ziesmer, Justina Venckute Larsson, and Georgios A. Sotiriou. "Hybrid microneedle arrays for antibiotic and near-IR photothermal synergistic antimicrobial effect against Methicillin-Resistant Staphylococcus aureus". In: *Chemical Engineering Journal* 462 (2023), p. 142127. DOI: https://doi.org/10.1016/j.cej.2023.142127.

[4] Daniel G. Meeker, Samir V. Jenkins, Emily K. Miller, Karen E. Beenken, Allister J. Loughran, Amy Powless, Timothy J. Muldoon, Ekaterina I. Galanzha, Vladimir P. Zharov, Mark S. Smeltzer, and Jingyi Chen. "Synergistic Photothermal and Antibiotic Killing of Biofilm-Associated Staphylococcus aureus Using Targeted Antibiotic-Loaded Gold Nanoconstructs". In: *ACS INFECTIOUS DISEASES* 2 (2016), pp. 241–250. DOI: https://doi.org/10.1021/acsinfecdis.5b00117.

[5] Danfeng He, Tao Yang, Wei Qian, Chao Qi, Li Mao, Xunzhou Yu, Huifeng Zhu, Gaoxing Luo, and Jun Deng. "Combined photothermal and antibiotic therapy for bacterial infection via acidity-sensitive nanocarriers with enhanced antimicrobial performance". In: *Applied Materials Today* 12 (2018), pp. 415–429. DOI: https://doi.org/10.1016/j.apmt.2018.07.006.

[6] Lingling Zhang, Yingqian Wang, Jie Wang, Yulan Wang, Aoying Chen, Can Wang, Wenting Mo, Yingxue Li, Quan Yuan, and Yufeng Zhang. "Photon-Responsive Antibacterial Nanoplatform for Synergistic Photothermal-/Pharmaco-Therapy of Skin Infection". In: *ACS Applied Materials & Interfaces* 11.1 (2019), pp. 300–310. DOI: 10.1021/acsami.8b18146.

[7] Jie Cao, Tong Sun, and Kenneth T.V. Grattan. "Gold nanorod-based localized surface plasmon resonance biosensors: A review". In: *Sensors and Actuators B: Chemical* 195 (2014), pp. 332–351. DOI: https://doi.org/10.1016/j.snb.2014.01.056.

[8] Y. Ozaki, T. Genkawa, and Y. Futami. "Near-Infrared Spectroscopy". In: *Encyclopedia of Spectroscopy and Spectrometry (Third Edition)*. Academic Press,

2017, pp. 40–49. DOI: https://doi.org/10.1016/B978-0-12-409547-2.12164-X.

[9] Alaaldin M. Alkilany, Lucas B. Thompson, Stefano P. Boulos, Patrick N. Sisco, and Catherine J. Murphy. "Gold nanorods: Their potential for photothermal therapeutics and drug delivery, tempered by the complexity of their biological interactions". In: *Advanced Drug Delivery Reviews* 64.2 (2012), pp. 190–199. DOI: https://doi.org/10.1016/j.addr.2011.03.005.

[10] Britannica Academic. *Staphylococcus*. https://academic-eb-com.eu1.proxy.openathens.net/levels/collegiate/article/staphylococcus/69433. Accessed: 2022-09-16. 2022.

[11] Raphael Saginur, Melissa StDenis, Wendy Ferris, Shawn D. Aaron, Francis Chan, Craig Lee, and Karam Ramotar. "Multiple Combination Bactericidal Testing of Staphylococcal Biofilms from Implant-Associated Infections". In: *Antimicrobial Agents and Chemotherapy* 50.1 (2006), pp. 55–61. DOI: 10.1128/AAC.50.1.55-61.2006.

[12] Robert J. Kadner and Kara Rodgers. *bacteria*. https://www.britannica.com/science/bacteria. Accessed: 2023-05-07. 2023.

[13] Mats Hulander, Håkon Valen-Rukke, and Martin Andersson. "Influence of Fibrinogen on Staphylococcus epidermidis Adhesion Can Be Reversed by Tuning Surface Nanotopography". In: *ACS biomaterials science & engineering* 5 (2019). DOI: https://doi.org/10.1021/acsbiomaterials.9b00450.

[14] Britannica Academic. *Antibiotic*. https://academic-eb-com.eu1.proxy.openathens.net/levels/collegiate/article/antibiotic/7811. Accessed: 2022-09-27. 2022.

[15] Britannica Academic. *Antibiotic Resistance*. https://academic-eb-com.eu1.proxy.openathens.net/levels/collegiate/article/antibiotic-resistance/473954. Accessed: 2022-09-28. 2021.

[16] Xiaohua Huang and Mostafa A. El-Sayed. "Gold nanoparticles: Optical properties and implementations in cancer diagnosis and photothermal therapy". In: *Journal of Advanced Research* 1.1 (2010), pp. 13–28. DOI: https://doi.org/10.1016/j.jare.2010.02.002.

[17] Britannica Academic. *Free-Electron Model of Metals*. https://academic-eb-com.eu1.proxy.openathens.net/levels/collegiate/article/free-electron-model-of-metals/35281. Accessed: 2022-09-28. 2006.

[18] Luigi La Spada and Lucio Vegni. "Electromagnetic Nanoparticles for Sensing and Medical Diagnostic Applications". In: *Materials (Basel)* 11 (2018), pp. 1944–1996. DOI: https://doi.org/10.3390/ma11040603.

[19] Ludovico Cademartiri and Geoffrey A. Ozin. "Gold". In: *Concepts of Nanochemistry*. Weinheim: WILEY-VCH GmbH & Co. KGaA, 2009, pp. 89–90.

[20] Minho Kim, Jung-Hoon Lee, and Jwa-Min Nam. "Plasmonic Photothermal Nanoparticles for Biomedical Applications". In: *Advanced Science* 6 (2019). DOI: https://doi.org/10.1002/advs.201900471.

[21] Ludovico Cademartiri and Geoffrey A. Ozin. "Gold". In: *Concepts of Nanochemistry*. Weinheim: WILEY-VCH GmbH & Co. KGaA, 2009, pp. 99–100.

[22] Leonardo Scarabelli, Ana Sánchez-Iglesias, Jorge Pérez-Juste, and Luis M. Liz-Marzán. "A "Tips and Tricks" Practical Guide to the Synthesis of Gold

Nanorods". In: *The Journal of Physical Chemistry Letters* 6 (2015), pp. 4270–4279. DOI: https://doi.org/10.1021/acs.jpclett.5b02123.

[23] H. K. Jang, Y. D. Chung, S. W. Whangbo, T. G. Kim, and C. N. Whang. "Effects of chemical etching with nitric acid on glass surfaces". In: *Journal of Vacuum Science & Technology* 19 (2001), pp. 267–274. DOI: https://doi.org/10.1116/1.1333087.

[24] Marwa Hameed AlKhafaji and Mohammed Hayder Hashim. "The synergistic effect of biosynthesized gold nanoparticles with antibiotic against clinical isolates". In: *Jornal of Biotechnology Research Center* 13 (2019), pp. 58–62. DOI: https://doi.org/10.24126/jobrc.2019.13.1.569.

[25] Syed Zeeshan Haider Naqvi, Urooj Kiran, Muhammad Ishtiaq Ali, Asif Jamal, Abdul Hameed, Safia Ahmed, and Naeem Ali. "Combined efficacy of biologically synthesized silver nanoparticles and different antibiotics against multidrug-resistant bacteria". In: *International Journal of Nanomedicine* 8 (2013), pp. 3187–3195. DOI: https://doi.org/10.2147/IJN.S49284.

[26] Yangzhouyun Xie, Wenfu Zheng, and Xingyu Jiang. "Near-Infrared Light-Activated Phototherapy by Gold Nanoclusters for Dispersing Biofilms". In: *ACS Applied Materials & Interfaces* 12 (2020), pp. 9041–9049. DOI: https://doi.org/10.1021/acsami.9b21777.

[27] Kyung-Suk Moon, Ji-Myung Bae, Sungho Jin, and Seunghan Oh. "Infrared-Mediated Drug Elution Activity of Gold Nanorod-Grafted $TiO_2$ Nanotubes". In: *Journal of Nanomaterials* 2014 (2014). DOI: https://doi.org/10.1155/2014/750813.

[28] Irith Wiegand, Kai Hilpert, and Robert E. W. Hancock. "Agar and broth dilution methods to determine the minimal inhibitory concentration (MIC) of antimicrobial substances". In: *Nature Protocols* 3 (2008), pp. 163–175. DOI: https://doi.org/10.1038/nprot.2007.521.

[29] Heinz-Helmut Perkampus. "Introduction". In: *UV-VIS Spectroscopy and Its Applications*. Heidelberg: Springer Berlin, 1992, pp. 1–2.

[30] Daniel C. Harris and Charles A. Lucy. "Fundamentals of Spectroscopy". In: *Quantitative Chemical Analysis*. New York, NY: W. H. Freeman and Company, 2020, pp. 443–463.

[31] Kalsoom Akhtar, Shahid Ali Khan, Sher Bahadar Khan, and Abdullah M. Asiri. "Scanning Electron Microscopy: Principle and Applications in Nanomaterials Characterization". In: *Handbook of Materials Characterization*. Cham: Springer International Publishing, 2018, pp. 113–145. DOI: 10.1007/978-3-319-92955-2_4.

[32] R.F. Egerton. "The Scanning Electron Microscope". In: *Physical principles of electron microscopy: An introduction to TEM, SEM, and AEM*. Cham: Springer International Publishing, 2016, pp. 121–147.

[33] Jurek W. Dobrucki and Ulrich Kubitscheck. "Fluorescence Microscopy". In: *Fluorescence Microscopy : From Principles to Biological Applications*. Weinheim: John Wiley & Sons, Incorporated, 2017, pp. 85–132.

[34] Julia Robertson, Cushla McGoverin, Frédérique Vanholsbeeck, and Simon Swift. "Optimisation of the Protocol for the LIVE/DEAD®BacLight™ Bacte-

rial Viability Kit for Rapid Determination of Bacterial Load". In: *Frontiers in Microbiology* 10 (2019). DOI: https://doi.org/10.3389/fmicb.2019.00801.

[35] O Ekici, R K Harrison, N J Durr, D S Eversole, M Lee, and A Ben-Yakar. "Thermal Analysis of Gold Nanorods Heated with Femtosecond Laser Pulses". In: *Journal of physics D: Applied physics* 41 (2008). DOI: https://doi.org/10.1088/0022-3727/41/18/185501.

# A

# Appendix

## A.1 Calculation of Theoretical Concentration of Purified Gold Nanorods

Theoretical calculations were performed to decide the concentration of the gold nanorods succeeding synthesis and purification.

Firstly, was the moles of Au(III) added to the seed solution decided, with origin from the gold precursor.

$$n_{Au(III)}^{seed\_solution} = 26 \cdot 10^{-6} l \cdot 50 \cdot 10^{-3} M = 1.25 \cdot 10^{-6} mole$$

95% of the Au(III) ions are assumed to be reduced in the seed solution, the concentration of Au(0) atoms can then be determined by knowing the total volume of the seed solution $V_{seed\_solution}$.

$$C_{Au(0)}^{seed\_solution} = \frac{0.95 \cdot n_{Au(III)}^{seed\_solution}}{V_{seed\_solution}} = \frac{0.95 \cdot 1.25 \cdot 10^{-6} mole}{5.025 \cdot 10^{-3} l} = 2.36 \cdot 10^{-4} M$$

The moles of Au(0) in 24 $\mu$l seed solution, added to the growth solution, was thereafter calculated.

$$n_{Au(0)}^{seeds} = 24 \cdot 10^{-6} l \cdot 2.36 \cdot 10^{-4} M = 5.67 \cdot 10^{-9} mole$$

Assumed that 95% of the Au(III) from the gold precursor present in the growth solution was reduced, the moles of Au(0) can then be decided.

$$n_{Au(0)}^{growth\_solution} = 0.95 \cdot 600 \cdot 10^{-6} l \cdot 50 \cdot 10^{-3} M = 2.85 \cdot 10^{-5} mole$$

The total amount of Au(0) present during the synthesis can thereafter be calculated.

$$n_{Au(0)}^{tot} = n_{Au(0)}^{growth\_solution} + n_{Au(0)}^{seeds} = 2.850567 \cdot 10^{-5} mole$$

The volume of Au(0) atoms was decided, where $M_{Au(0)}$ is the molar mass of gold.

$$V_{Au(0)} = \frac{n_{Au(0)}^{tot} \cdot M_{Au(0)}}{\rho_{Au(0)}} = \frac{2.850567 \cdot 10^{-5} mole \cdot 196.97 \frac{g}{mole}}{19.3 \cdot 10^{-6} \frac{g}{m^3}} = 2.91 \cdot 10^{-10} m^3$$

The volume of gold nanorods was then calculated based on the average length and width presented in table 4.1, where $w$ is the width and $l$ is the length. The nanorods were assumed to have the shape of a cylinder.

$$V_{AuNR} = \pi \cdot l(\frac{w}{2})^2 = \pi \cdot 64 \cdot 10^{-6} nm(\frac{20.6 \cdot 10^{-9} nm}{2})^2 = 2.13 \cdot 10^{-23} m^3$$

The theoretical amount of nanorods in moles can then be determined, where $N_A$ is Avogadro's constant.

$$n_{AuNR} = \frac{V_{Au(0)}}{V_{AuNR} \cdot N_A} = \frac{2.91 \cdot 10^{-10} m^3}{2.13 \cdot 10^{-23} m^3 \cdot 6.022 \cdot 10^{23} \frac{1}{mole}} = 2.27 \cdot 10^{-11} mole$$

The concentration of nanorods could succeedingly be determined by knowing the total volume of the synthesis solution $V_{synthesis\_solution}$.

$$n_{AuNR} = \frac{n_{AuNR}}{V_{synthesis\_solution}} = \frac{2.27 \cdot 10^{-11} mole}{4 \cdot 10^{-3} l} = 5.68 \cdot 10^{-9} M$$

Three purification steps were thereafter performed to remove remainings from the synthesis. 80% of the gold nanorods were assumed to remain after each purification step. Lastly, the final concentration of gold nanorods was calculated.

$$C_{AuNR\_final} = 0.8^3(5.68 \cdot 10^{-9} M) = 2.91 \cdot 10^{-9} M \approx 3 \cdot 10^{-9} M$$

## A.2 Fluorescence Microscopy Images for Photothermal Elimination of Bacteria

This section shows single channel fluorescence microscopy images when evaluating the antimicrobial activity of the gold nanorods exposed to NIR-light. Two systems were evaluated; the gold nanorods irradiated covered with a thin liquid film and immersed in liquid.

### A.2.1 Irradiation while Covered with Thin Liquid Film

Figure A.1 shows single channel microscopy images of *S. aureus* on gold nanorod-functionalised glass covered with a thin liquid film during irradiation, both after irradiation with 24 W/cm$^2$ for 10 s and without irradiation. The amount of live bacteria is represented by the green channel and the amount of dead bacteria by the red channel.

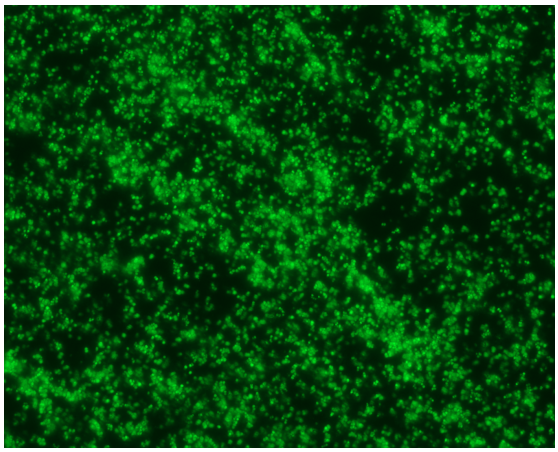

**(a)** NIR-light.

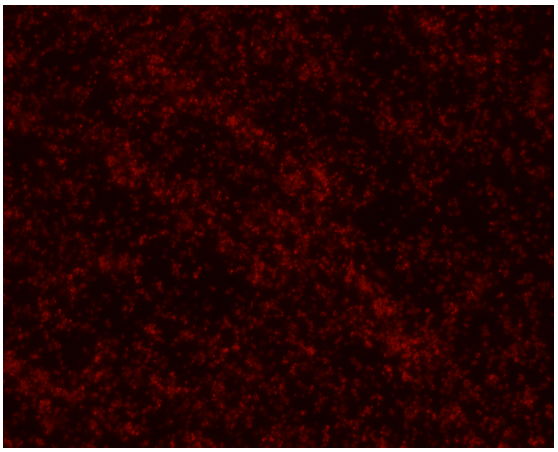

**(b)** NIR-light.

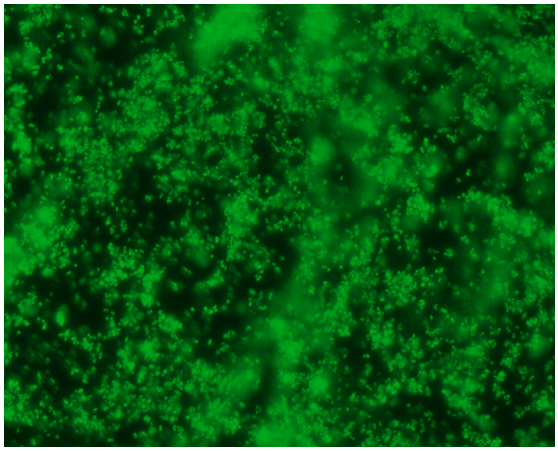

**(c)** No NIR-light.

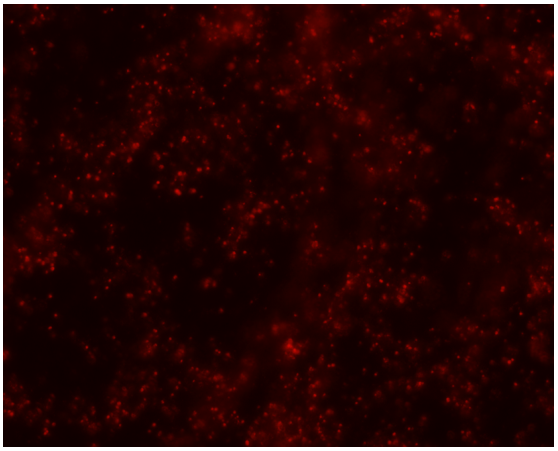

**(d)** No NIR-light.

**Figure A.1:** Microscope images of *S. aureus* on gold nanorod-functionalised glass covered with a thin liquid film during irradiation. (a) Live bacteria after irradiation with 24 W/cm$^2$ for 10 s, (b) dead bacteria after irradiation with 24 W/cm$^2$ for 10 s, (c) live bacteria with no NIR exposure and (d) dead bacteria bacteria with no NIR exposure.

### A.2.2 Irradiation while Immersed in Liquid

Figure A.2 shows single channel microscopy images of *S. aureus* on gold nanorod-functionalised glass immersed in 1 ml PBS during irradiation, both after irradiation with 24 W/cm$^2$ for 10 s and without irradiation. The amount of live bacteria is represented by the green channel and the amount of dead bacteria by the red channel.

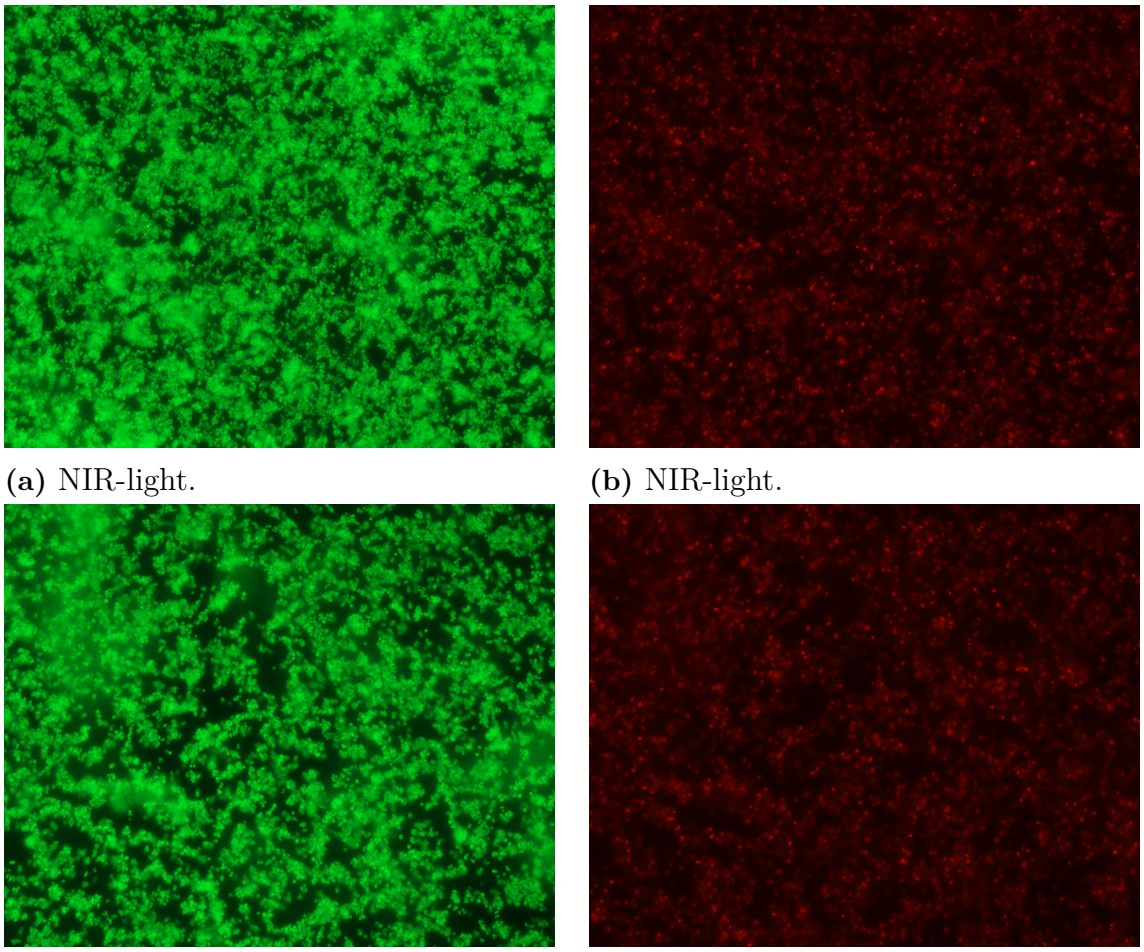

**(a)** NIR-light.

**(b)** NIR-light.

**(c)** No NIR-light.

**(d)** No NIR-light.

**Figure A.2:** Microscope images of *S. aureus* on gold nanorod-functionalised glass immersed in liquid during irradiation. (a) Live bacteria after irradiation with 24 W/cm$^2$ for 10 s, (b) dead bacteria after irradiation with 24 W/cm$^2$ for 10 s, (c) live bacteria with no NIR exposure and (d) dead bacteria with no NIR exposure.

## A.3 Fluorescence Microscopy Images for MIC Determination of Surface Grown Bacteria

Figure A.3 shows single channel microscopy images of *S. aureus* on gold nanorod-functionalised glass after incubation in various concentrations of vancomyicin for 18 h. The concentrations investigated were 0 mg/l, 1 mg/l, 2 mg/l, 3 mg/l and 4 mg/l. The amount of live bacteria is represented by the green channel and the amount of dead bacteria by the red channel.

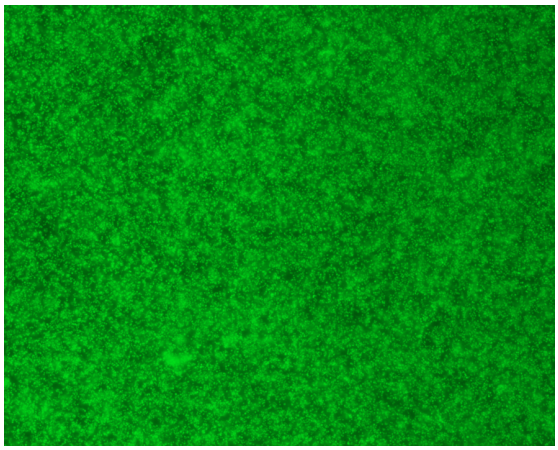

**(a)** 0 mg/l.

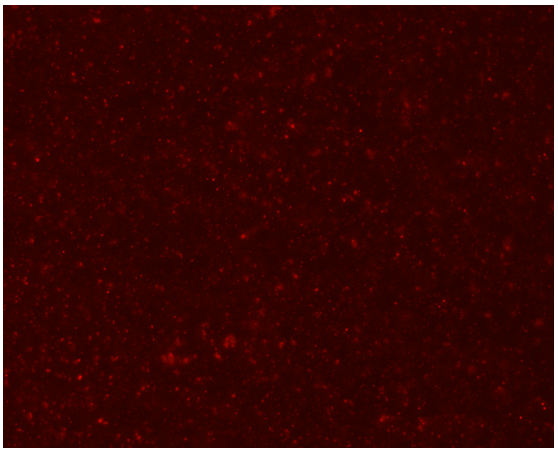

**(b)** 0 mg/l.

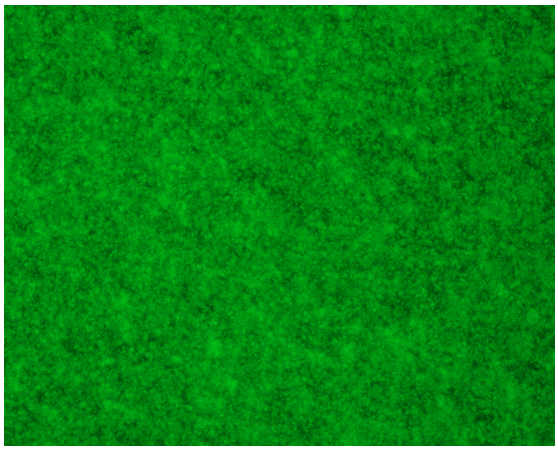

**(c)** 1 mg/l.

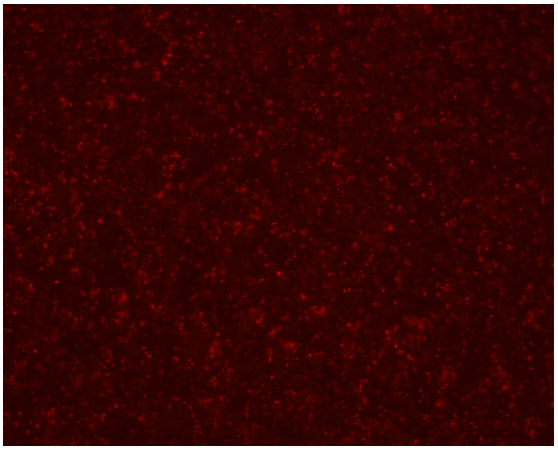

**(d)** 1 mg/l.

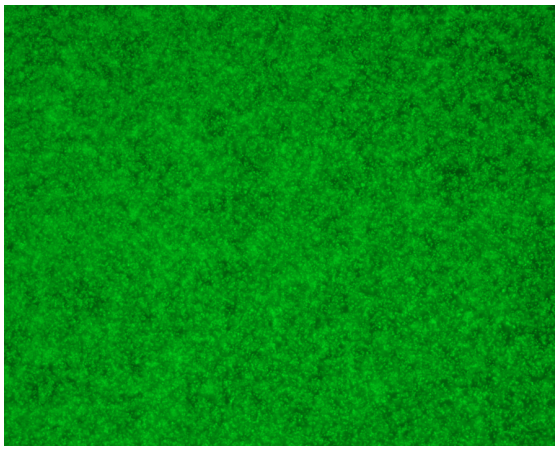

**(e)** 2 mg/l.

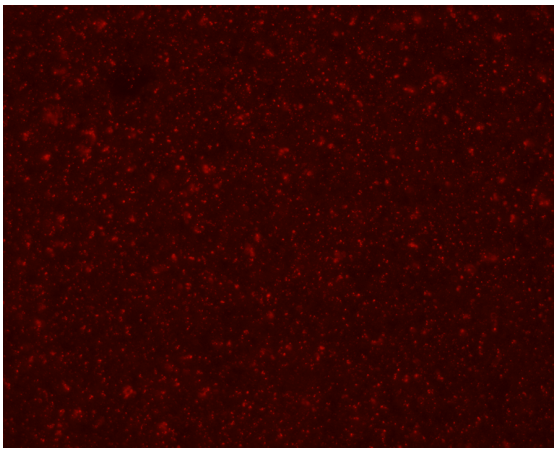

**(f)** 2 mg/l.

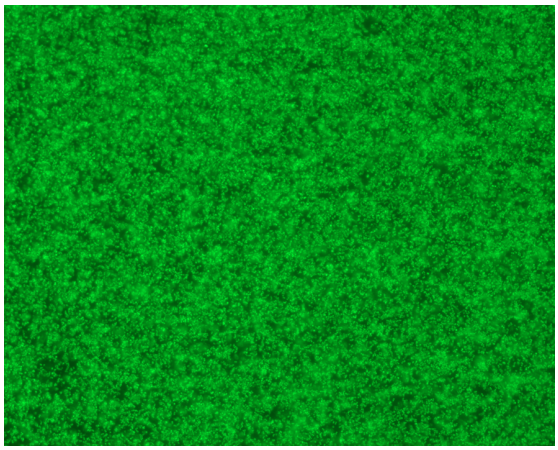

**(g)** 3 mg/l.

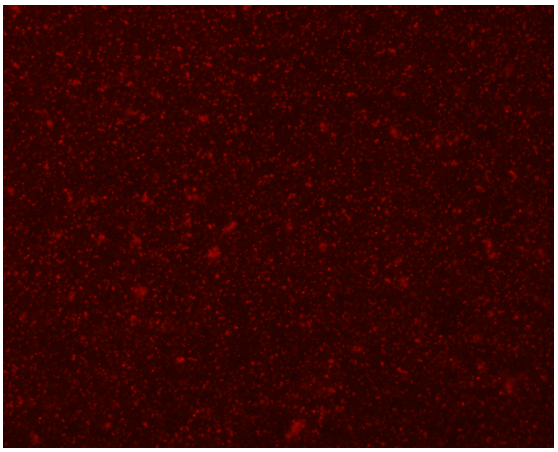

**(h)** 3 mg/l.

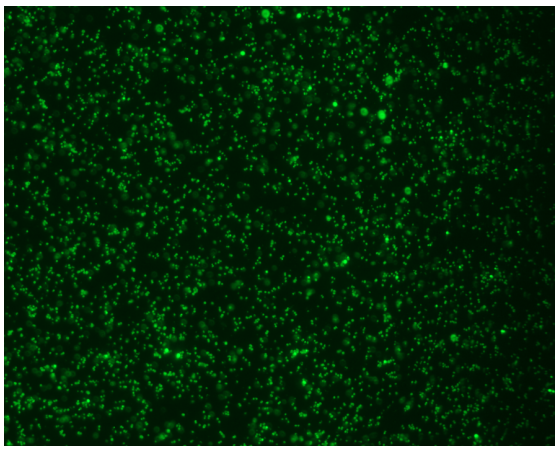

**(i)** 4 mg/l.

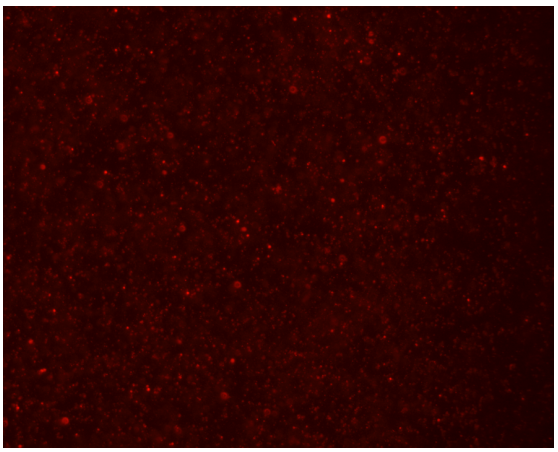

**(j)** 4 mg/l.

**Figure A.3:** Microscope images of *S. aureus* on gold nanorod-functionalised glass incubated in various concentrations of vancomycin for 18 h. (a) Live bacteria when incubated without vancomycin, (b) dead bacteria when incubated without vancomycin, (c) live bacteria when incubated in 1 mg/l, (d) dead bacteria when incubated in 1 mg/l, (e) live bacteria when incubated in 2 mg/l. (f) dead bacteria when incubated 2 mg/l, (g) live bacteria when incubated in 3 mg/l, (h) dead bacteria when incubated in 3 mg/l, (i) live bacteria when incubated in 4 mg/l and (j) dead bacteria when incubated in 4 mg/l.

## A.4 Fluorescence Microscopy Images when Combining Photothermal Elimination and Antibiotics

Figure A.4 shows single channel microscopy images of *S. aureus* on gold nanorod-functionalised glass immersed in 600 $\mu$l antibiotic solution during irradiation and thereafter incubated for 18 h. One sample group was irradiated with 3 W/cm$^2$ for 1 min and incubated without vancomycin, one was incubated in 3 mg/l vancomycin and the last was irradiated with 3 W/cm$^2$ for 1 min and incubated in 3 mg/l van-

comycin. The amount of live bacteria is represented by the green channel and the amount of dead bacteria by the red channel.

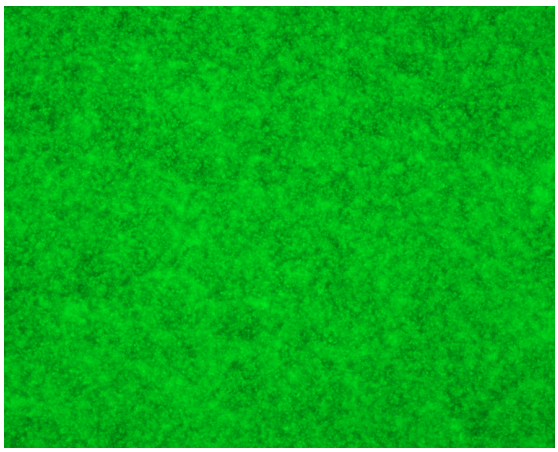

**(a)** NIR-light.

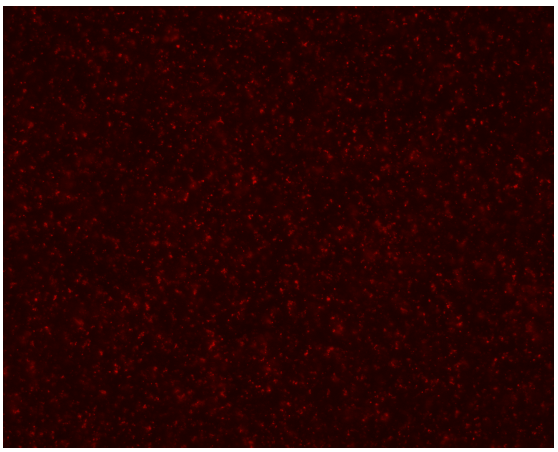

**(b)** NIR-light.

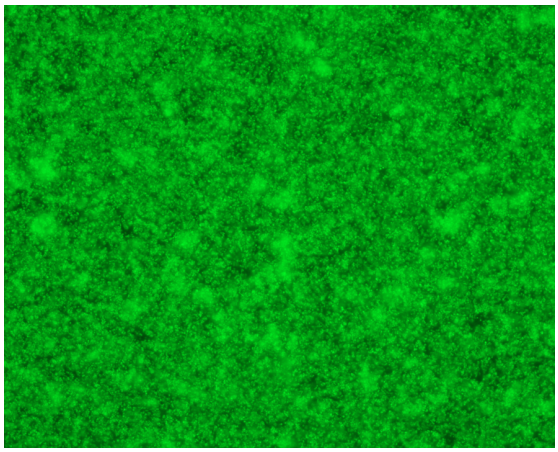

**(c)** Vancomycin.

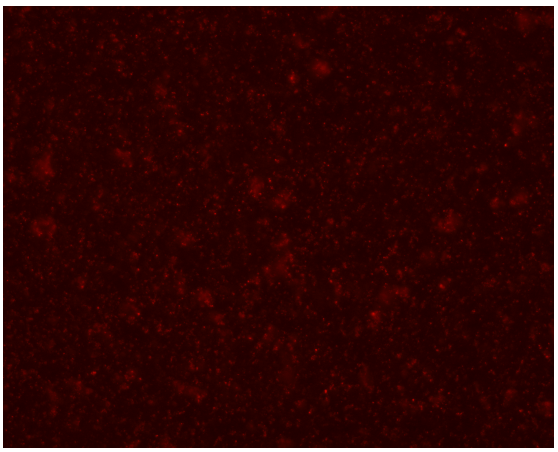

**(d)** Vancomycin.

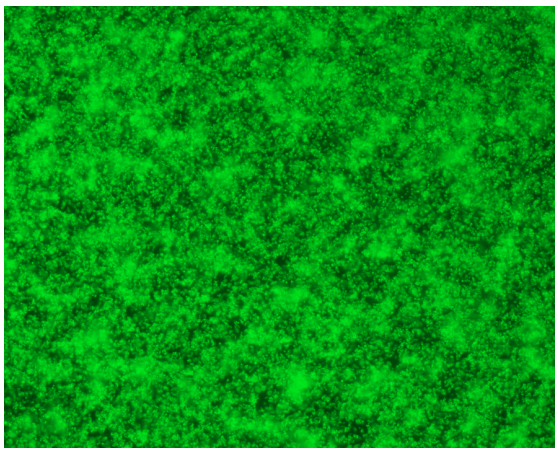

**(e)** NIR-light + Vancomycin.

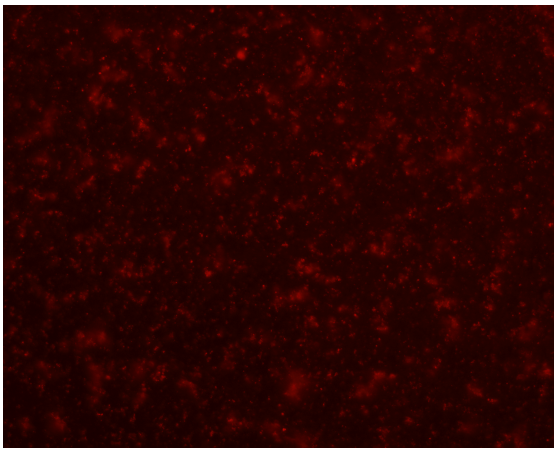

**(f)** NIR-light + Vancomycin.

**Figure A.4:** Microscope images of *S. aureus* on gold nanorod-functionalised glass immersed in liquid during irradiation and thereafter incubated for 18 h. (a) Live bacteria after irradiation with of 3 W/cm$^2$ for 1 min, (b) dead bacteria after irradiation with 3 W/cm$^2$ for 1 min, (c) live bacteria after incubation in 3 mg/l vancomycin, (d) dead bacteria after incubation in 3 mg/l vancomycin, (e) live bacteria after irradiation with 3 W/cm$^2$ for 1 min and incubation in 3 mg/l vancomycin, (f) dead bacteria after irradiation with 3 W/cm$^2$ for 1 min and incubation in 3 mg/l vancomycin.

**DEPARTMENT OF CHEMISTRY AND CHEMICAL ENGINEERING**
**CHALMERS UNIVERSITY OF TECHNOLOGY**
Gothenburg, Sweden
www.chalmers.se


CHALMERS
UNIVERSITY OF TECHNOLOGY